scientific reports

Check for updates

OPEN

UV-C irradiation enhances the antimicrobial and Anti-Inflammatory bioactivity of ginseng oil

Aisha M. H. Al-Rajhi[1], Sulaiman A. Alsalamah[2]✉, Abdullah M. Almotayri[3], Nourah M. Almimoni[3], Reham Yahya[4,5], Asmaa A. Alharbi[6] & Mashael Hakami[7]

The use of medicinal plants as an effective source of therapeutic compounds has become increasingly urgent due to the spread of serious diseases, particularly those caused by resistant pathogenic bacteria. In this study, the bioactivity of ginseng oil extract exposed to ultraviolet (UV-C) radiation for 0, 30, and 60 min was evaluated. Ginseng oil extract exhibited potent antimicrobial activity against *Bacillus subtilis*, *Staphylococcus aureus*, *Klebsiella pneumoniae*, *Salmonella typhi*, and *Candida albicans*, but not *Aspergillus niger* at 0, 30, and 60 min. The MICs of the ginseng oil extract after UV-C exposure at 0, 30, and 60 min were 125, 62.5, and 31.25 µg/ml for *B. subtilis;* 125, 125, and 62.5 µg/ml for *S. aureus;* 250, 125, and 31.25 µg/ml for *K. pneumoniae;* 125, 62.5, and 15.62 µg/ml for *S. typhi;* 62.5, 15.62 and 15.62 µg/ml for *C. albicans*, respectively. Ginseng oil extract exposed to UV-C for 60 min showed the lowest MBC values compared to exposure at 0 and 30 min. Different concentrations of ginseng oil extract showed anti-inflammatory activity compared to sodium dodecyl sulfate as a standard, in addition to anti-biofilm activity compared to blank and control at different time intervals of UV-C exposure. Based on GC-MS analysis, ginseng oil extract contains 24 components for 0 and 30 min, while it contains 29 components for 60 min. The dominant components are hexadecanoic acid methyl ester; 9,12-octadecadienoyl chloride; n-hexadecanoic acid; 9,12-octadecadienoic acid (Z, Z) methyl ester; 9-octadecenoic acid ethyl ester; 9,12-octadecadienoic acid; 9-octadecenoic acid; oleic acid; 9,12-octadecadienoic acid (Z, Z)-; 2-hydroxy-1-(hydroxymethyl) ethyl ester; and (+)-Sesamin. Different concentrations of ginseng oil extract exhibited anti-inflammatory activity compared with sodium dodecyl sulfate (standard), as well as anti-biofilm activity relative to blank and untreated controls across the various UV-C exposure times.

Keywords Ginseng; extraction, Volatile oil, Biofilm, Antimicrobial activity, GC-MS analysis

Natural products extracted from medicinal plants still play an important role in the medical field as alternative medicine. Many of these products are widely used as active ingredients in the pharmaceutical industry. In the past century, a wide range of serious diseases have emerged and spread widely throughout the world, including infectious diseases, including enterocolitis, and non-infectious diseases, including cardiovascular diseases and inflammation[1]. Some microbes, especially bacteria, are developing resistance to multiple drugs, which is a major clinical problem and causes high rates of mortality and morbidity worldwide. Multidrug-resistant Gram-positive and Gram-negative bacteria represent a major clinical problem, especially in developing countries, due to their ability to resist multiple antibiotics at high concentrations and overdoses, causing death. As reported in several WHO reports, high mortality rates among children, especially in developing countries, have been recorded due

[1]Department of Biology, College of Science, Princess Nourah bint Abdulrahman University, P.O. Box 84428, Riyadh 11671, Saudi Arabia. [2]Department of Biology, College of Science, Imam Mohammad Ibn Saud Islamic University (IMSIU), Riyadh 11623, Saudi Arabia. [3]Department of Biology, Faculty of Science, Al-Baha University, 65779 Al-Baha, Saudi Arabia. [4]Basic Sciences Department, College of Science and Health Professions, King Saud bin Abdulaziz University for Health Sciences, Riyadh 11481, Kingdom of Saudi Arabia. [5]King Abduallah International Medical Research Center, King Saud Bin Abdulaziz University for Health Sciences, P.O. Box 3660, Riyadh 11481, Saudi Arabia. [6]Department of Biology, College of Science, Jazan University, P.O. Box. 114, Jazan 45142, Saudi Arabia. [7]Pharmacy Department, Jazan University Hospital, Jazan University, Jazan, Saudi Arabia. ✉email: SAAlsalamah@imamu.edu.sa

to multidrug-resistant bacteria resulting from the misuse of antibiotics[2]. Therefore, it was necessary to search for effective alternatives to antibiotics that had become ineffective against these resistant and fierce bacteria. It was urgent to resort to medicinal plants to extract highly effective natural antibiotics to control these bacteria that use multiple mechanisms to resist many antibiotics[3].

Panax ginseng is a perennial herb belonging to the family Araliaceae and is one of the effective medicinal plants. The word *Panax* is derived from the Greek word panacea, which means cure for all diseases, so the name ginseng refers to its broad therapeutic properties that treat many conditions[4]. The genus *Panax* is widely cultivated throughout the world, especially in Asia, the United States, and Canada, and includes 17 species, including *P. ginseng*, *P. quinquefolius*, *P. notoginseng*, *P. japonicus*, and *P. vietnamensis*[5]. *P. ginseng* contains various therapeutic and nutritional components, including ginsenosides, polysaccharides, amino acids, volatile oils, organic acids, and trace elements[6]. Ginsenosides are the most therapeutic components, as they are polysaccharide derivatives consisting of hemiacetal hydroxyl groups of sugar and non-sugar compounds. Ginsenosides are classified into three main groups based on chemical structure, namely protopanaxadiol, protopanaxatriol, and oleanolan, and these groups include more than 180 ginsenosides, for instance Rh1, Rb1, Rc, Rb2, Rd, Re, and Rg1, which account for 90% of the total ginsenosides[7]. These ginsenosides are used to treat various conditions, including neurological diseases[8], diabetes, and cardiovascular diseases[9].

Although inflammation is a fundamental response to control and eliminate all foreign bodies including pathogens that attack the human body, it must be treated to prevent its harmful effects that affect vital processes[10]. *P. ginseng* is widely used as a powerful anti-inflammatory due to its content of various therapeutic components, including ginsenosides, acid glucan, glycopeptides, phytosterols, and polyacetylenes that effectively treat serious inflammations in different parts of the body[11]. Ginseng roots contain various components that have broad-spectrum therapeutic activities, including anti-inflammatory effects[12]. Chinese ginseng is an effective traditional medicine that treats many serious diseases, including gastrointestinal colitis. Therefore, it has been developed as a potent anti-inflammatory and immunomodulatory drug[6]. Ginseng roots contain effective therapeutic components, including ginsenosides, ginseng polysaccharide, and ginseng polypeptides that treat serious inflammations as harmful threats to human health. The ginsenosides in American ginseng are F11, Rb1, Re, Rd, Rc, Rg1, and Rb3, while those in Asian ginseng are Rb2, Rf, Rb1, Rc, Rd, Re, and Rg1, and those in *P. notoginseng* are Rg1, Rb1, and Rd, not ginsenoside R1, which provide promising effects in the treatment of various diseases, including cardiovascular diseases[13]. Ginseng total saponins effectively reduce RBCs hemolysis, even at low concentrations of hydrogen peroxide. They exert protective effects on RBCs by improving cell shape, enhancing oxygen-carrying capacity, promoting membrane protein expression, and stimulating the activities of antioxidant enzymes, ATPase, and intracellular ATP levels[14].

Pathogenic bacteria, especially those that form biofilms, represent a major problem, as they defend themselves against various antibiotics and thus cause serious diseases. For example, *Porphyromonas gingivalis*, an anaerobic Gram-negative bacterium, causes periodontal disease and resistance to various antibiotics due to its ability to form biofilms on oral tissues using a quorum sensing mechanism in which communication between bacterial cells is developed[15]. *P. gingivalis* produces acylated homoserine lactones (AHLs) that are responsible for the signaling function in the quorum sensing mechanism. Therefore, the treatment of periodontitis depends on stopping the production of AHLs[16]. *P. ginseng* exhibits various therapeutic effects, including antibacterial, anti-biofilm, and anti-inflammatory activities, as it contains ginsenosides and saponins, which can inhibit the quorum sensing mechanism and biofilm production[17]. Nowadays and in the future, the extraction of therapeutic components from medicinal plants by less expensive mechanisms greatly enhances the pharmaceutical industry, providing highly effective and inexpensive drugs with limited side effects. The emergence of multidrug-resistant microorganisms has deepened the exploration for novel natural therapeutics. Although ginseng and its oil extracts are well-documented for diverse pharmacological properties, there is limited information about how UV-C irradiation can modify the chemical profile of ginseng oil and subsequently improve its biological activities. Prior studies have largely focused on crude oil without exploring the impact of controlled UV-C exposure on bioactivity. This investigation management this gap by investigate the effect of UV-C treatment on biological activities and phytochemical composition of ginseng oil extract. Therefore, this study aims to demonstrating the effect UV-C on the extract of ginseng oil and identify its therapeutic components that are used as antibacterial, antibiofilm, and anti-inflammatory.

Materials and methods

Plant materials

Ginseng seed oil was collected from Natural Food Choice Co. (Jeddah, Saudi Arabia). All media, reagents, and solvents were procured from Sigma-Aldrich (St. Louis, MO, USA).

Ginseng seed oil extraction

The endosperm portion of ginseng seeds was roasted at 200 °C for 30 min, then roasted ginseng seed was pressed using a screw-type oil sampler to extract the oil by pressing and then centrifuged at 8000 rpm for 20 min to remove impurities and obtain ginseng seed oil. Ginseng seed oil extraction was performed using and supercritical fluid extraction (SFE-(Hyeondae Green Industry, Seoul, Korea) at 150 bar/35°C for 60 min[18]. The prepared ginseng oil extract (GOE) was split into three equal volumes (50 ml/each) in three containers which were exposed to 18.0 mJ/cm^2 UV-C (254 nm) radiation at room temperature (28 °C). For varying amounts of time—0, 30, and 60 min, respectively[19].

In vitro assay of antimicrobial activity

The antimicrobial activity was tested in vitro using the agar well diffusion method at different time intervals (0-time, 30 min, and 60 min)[20]. Nutrient agar (Difco) and Sabouraud agar (Difco) were used with bacterial and

fungal strains, respectively (*B. subtilis* ATCC 6633, *S. aureus* ATCC 6538, *K. pneumoniae* ATCC 13883, *S. typhi* ATCC 6539, *C. albicans* ATCC 10221 and *A. niger* ATCC 16888), and the seeded plates were stored at 4°C for 1 h to demonstrate microbial growth. The test extract (100 µl) was inoculated into wells punched into the agar surface (6–8 mm) using a sterile cork punch, and the plates were incubated at 30 °C for 24 h and 72 h for bacteria and fungi, respectively. The appearance of an inhibition zone around the wells, which can be measured in mm, indicates antimicrobial activity. Negative controls were plates seeded with bacterial and fungal strains without test extract. Positive controls for bacteria were plates seeded with bacterial strains and gentamycin (1 mg/ml), while positive controls for fungi were plates seeded with fungal strains and fluconazole (1 mg/ml).

Determination of mics

Minimum Inhibitory Concentrations (MICs) were determined at different time intervals (0-time, 30 min, 60 min) using the microdilution method in which Mueller-Hinton broth was used[21]. The extracts were serially diluted two-fold to obtain a wide range of concentrations (0.98 to 1000 µg/ml). The wells of polystyrene microtiter plates were inoculated with 200 µl of the most suitable dilution of the tested extract mixed with broth medium. The microbial inoculum was prepared from fresh cultures dispensed in sterile 0.85% NaCl solution to meet McFarland turbidity standard (1 and 2 µl). This inoculum was inoculated into wells to obtain a density of 3×10^6 cfu/ml. MICs were determined after 72 h of incubation at 35 °C under microaerophilic conditions (15% CO_2). Plates seeded with extract-free microbial inoculation represented a positive control, and plates inoculated with serial folded double dilution extract (0.98–1000 µg/ml) without microbial inoculation represented a negative control. Turbidity was measured at 630 nm using a Biotech 800 TS microplate reader. Compare the amount of growth in the wells containing the extract to the amount of growth in the growth control wells (no extract) and the negative control wells used in each set of tests when determining growth endpoints. For the test to be considered valid, acceptable growth must occur in the growth-control well.

Determination of MBCs

Minimum bactericidal concentrations (MBCs) were determined by growing a microbial culture (100 ml) from each well that showed complete inhibition of growth, from the last positive and from the growth control, on Mueller Hinton agar plates. Plates were incubated at 35 °C for 72 h under microaerophilic conditions[21].

In vitro assay of anti-inflammatory activity

Fresh three mL of healthy blood (The blood sample used in this study was obtained from the corresponding author, who volunteered as a healthy donor specifically for this experiment) was injected into heparinized tubes and centrifuged at 3000 × g for 10 min. The RBCs pellets were dissolved using saline solution in the same volume as the supernatant. The resulting thawed RBCs were pelletized and reconstituted as a 40% v/v suspension with isotonic buffer solution (10 mM sodium phosphate buffer, 0.2 g NaH_2PO_4, 1.15 g Na_2HPO_4, 9 g NaCl, 1.0 L distilled water, pH 7.4). Reconstituted RBCs (resuspended supernatant) were used in this manner[22]. Hemolysin activities were tested in samples at sub-MICs (25%, 50%, and 75%) treated with bacteria[23]. Test bacteria treated with 25%, 50%, and 75% of the MIC (sub-MIC) or untreated cultures were adjusted to an OD_{600} of 0.4, and centrifuged at 21,000 × g for 20 min. The supernatant (500 µl) was added to fresh erythrocyte suspension (2%) in 0.8 ml of saline, incubated for 2 h at 37 °C and centrifuged at 11,000 × g for 10 min at 4 °C. A positive control (complete hemolysis) was prepared by adding 0.1% sodium dodecyl sulfate (SDS) to the RBC suspension and a negative control of non-hemolyzed RBC was prepared by incubating RBCs in LB broth under the same conditions. Hemoglobin release was assessed by determining the absorbance at 540 nm (triplicates). Hemolysis that occurred in cultures treated with MICs below the mean was presented as the mean ± standard error of the percentage change from hemolysis in untreated control cultures. Released hemoglobin was compared with positive and negative controls and the hemolysis rate was calculated using the formula:

$$\textbf{Hemolysis } (\%) = \frac{\mathbf{A_1} - \mathbf{A_2}}{\mathbf{A_3} - \mathbf{A_2}} \times 100$$

Where, A_1 is the absorbance of sample with bacterial culture, A_2 is the absorbance of negative control, and A_3 is the absorbance of positive control.

Microtiter plate assay for biofilm quantification

The effect of extracts on biofilm formation was evaluated in 96-well polystyrene flat-bottom plates[24]. Briefly, 300 µl of fresh trypticase-inoculated soy yeast (TSY) broth (final concentration 10^6 cfu/ml) was aliquoted into each well of the microplate and cultured in the presence of previously determined non-lethal concentrations (75%, 50%, and 25% of MBCs). Wells containing medium and those without extracts and containing only methanol were used as controls. The plates were incubated at 37°C for 48 h. After incubation, the supernatant was removed and each well was washed thoroughly with sterile distilled water to remove free floating cells. After this, the plates were air dried for 30 min and the formed biofilm was stained for 15 min at room temperature with 0.1% aqueous solution of crystal violet. After incubation, excess dye was removed by washing the plate three times with sterile distilled water. Finally, the cell-bound dye was solubilized by adding 250 µl of 95% ethanol to each well, and after 15 min of incubation, the absorbance was measured using a microplate reader at a wavelength of 570 nm[24].

$$\textbf{Biofilm inhibition } (\%) = 1 - \frac{\mathbf{A_s} - \mathbf{A_b}}{\mathbf{A_c} - \mathbf{A_b}} \times 100$$

where, A_s is the absorbance of sample, A_b is the absorbance of blank, and A_c is the absorbance of control.

GC-MS analysis

The chemical composition of the sample was determined at different time intervals (0-time, 30 min, 60 min) using a Trace GC1310-ISQ mass spectrometer (Thermo Scientific, Austin, TX, USA) with a TG–5MS direct capillary column (film thickness 30 m × 0.25 mm × 0.25 µm). The column oven temperature was initially held at 35 °C and then increased by 3 °C/min to 200 °C for 3 min and then increased to the final temperature of 280 °C by 3 °C/min and held for 10 min. The temperature of the injector and MS transfer line was maintained at 250 °C and 260 °C, respectively. Helium was used as the carrier gas at a constant flow rate of 1 ml/min. The solvent delay was 3 min and 1 µl diluted samples were automatically injected using the Autosampler AS1300 coupled to the GC in split mode. EI mass spectra were collected at an ionization voltage of 70 eV over the range of 40 to 1000 m/z in full scan mode. The ion source temperature was set at 200 °C. The components were identified by comparing their retention times and mass spectra with those in the WILEY 09 and NIST 11 mass spectra databases[25–28].

Statistical analysis

Statistical studies related to frequencies to calculate mean values ± standard deviation (SD) and mean values ± standard error (SE) using Microsoft Excel 365 and SPSS v.25. Quantitative data with standard distribution among different treatments were analyzed using one-way analysis of variance (ANOVA) and Tukey's post hoc test, at a probability level of 0.05.

Results and discussion

In vitro assay of antimicrobial activity

The antimicrobial activity of ginseng oil extract (GOE) was tested against two strains of Gram-positive bacteria (*B. subtilis* ATCC 6633 and *S. aureus* ATCC 6538), two strains of Gram-negative bacteria (*K. pneumoniae* ATCC 13883 and *S. typhi* ATCC 6539), and two strains of molds (*C. albicans* ATCC 10221 and *A. niger* ATCC 16888) at three-time intervals of exposure to UV-C at 0-time, 30 min, 60 min). GOE has shown broad-spectrum antimicrobial activity, inhibiting both Gram-positive and Gram-negative bacteria, as well as *C. albicans*, the most common infectious mold in humans, but it did not affect *(A) niger*. GOE showed the greatest inhibitory activity against *C. albicans*, followed by Gram-positive and Gram-negative bacteria, although there were slight differences (Fig. 1). GOE inhibited *(B) subtilis* with zones of inhibition measuring 16 ± 1.0, 20 ± 1.0, and 23 ± 1.0 mm at 0 min, 30 min, and 60 min of UV-C exposure, respectively, compared to 22 ± 1.0 mm for gentamicin as a positive control (Fig. 2A). GOE inhibited *S. aureus* with zones of inhibition measuring 17 ± 1.0, 17 ± 1.0, and 19 ± 1.0 mm at 0 min, 30 min, and 60 min of UV-C exposure, respectively, compared to 21 ± 1.0 mm for gentamicin as a positive control (Fig. 2B). GOE inhibited *K. pneumoniae* at 16 ± 1.0, 16 ± 2.0, and 20 ± 2.0 for 0-time, 30 min, and 60 min, respectively, compared to 20 ± 2.0 for gentamycin (Fig. 2C). GOE inhibited *S. typhi* at 15 ± 2.0, 18 ± 1.0, and 26 ± 1.0 for 0-time, 30 min, and 60 min, respectively, compared to 20 ± 1.0 for gentamycin (Fig. 2D). GOE

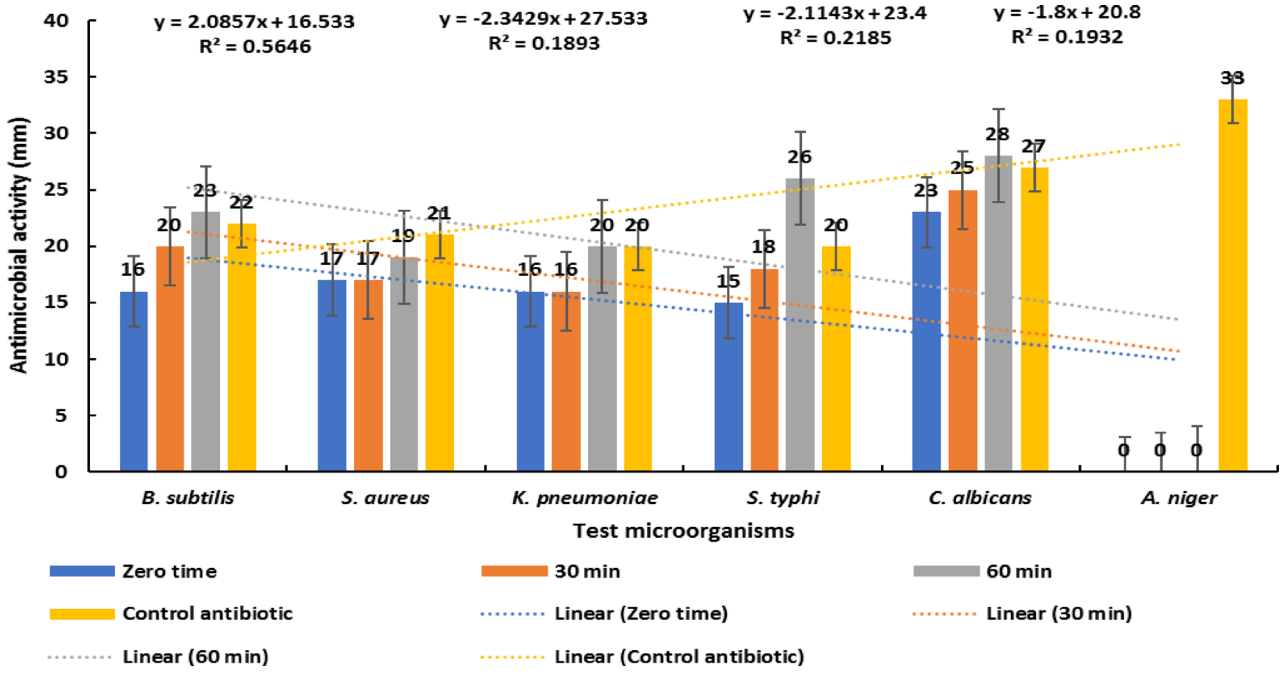

Fig. 1. Antimicrobial activity of GOE at different time intervals against different pathogens (A notable rise with non-significant difference $P > 0.05$ in antimicrobial action versus tested microbes upon increase time of exposure to UV-C; Data are represented as means ± SD).

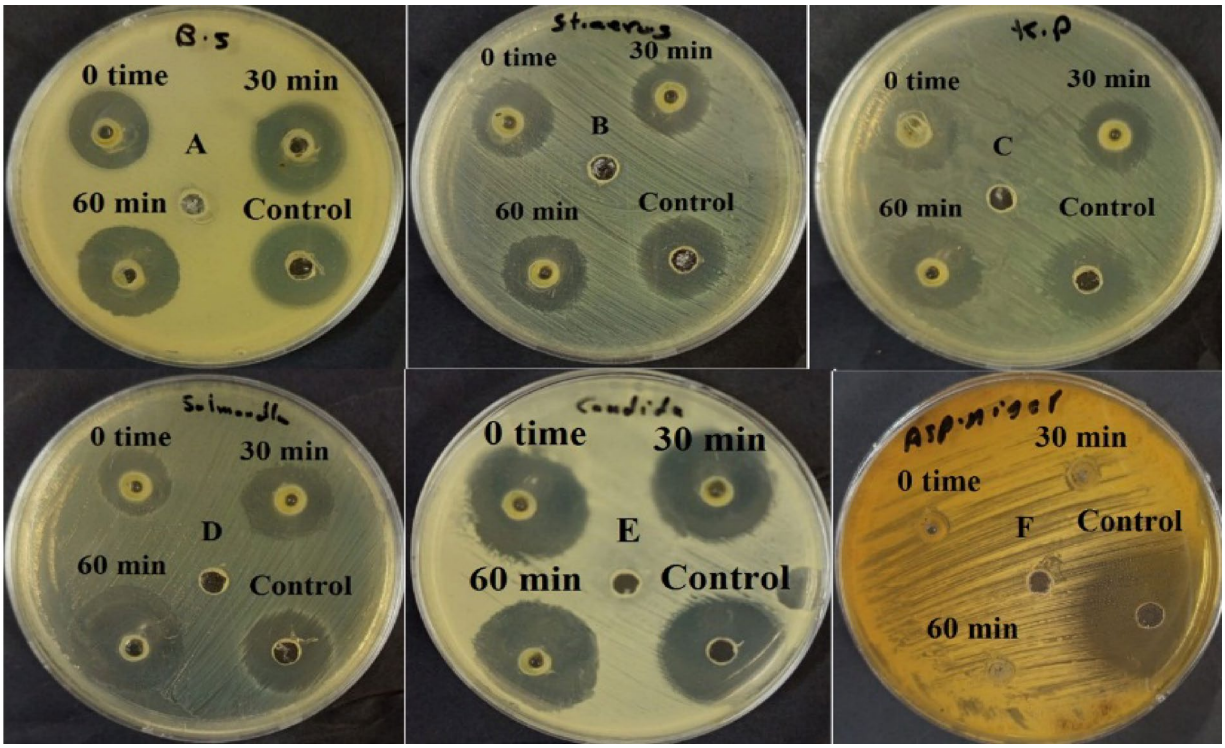

Fig. 2. Antimicrobial activity of GOE at different time intervals against: (A) *B. subtilis*, (B) *S. aureus*, (C) *K. pneumoniae*, (D) *S. typhi*, (E) *C. albicans*, and (F) *A. niger*.

inhibited *(C) albicans* at 23 ± 1.0, 25 ± 1.0, and 28 ± 1.0 for 0-time, 30 min, and 60 min, respectively, compared to 27 ± 3.0 for fluconazole as a positive control (Fig. 2E). GOE could not inhibit *A. niger* at all the time intervals, compared to 23 ± 3.0 for fluconazole (Fig. 2F). Thus, GOE exposed to UV-C for 60 min exhibited the highest antimicrobial activity, outperforming GOE at 0 and 30 min as well as gentamicin. GOE at 30 min showed greater antimicrobial activity than GOE at 0 min.

Wang et al.[29] reported that the three common ginseng species (*P. ginseng*, *P. quinquefolius*, and *P. notoginseng*) showed broad-spectrum antimicrobial activity against pathogenic Gram-negative bacteria (*P. aeruginosa*, *H. pylori*, and *E. coli*), pathogenic Gram-positive bacteria (*S. aureus* and *P. acnes*), and pathogenic fungi (*C. albicans* and *F. oxysporum*), due to their high contents of ginsenosides, polysaccharides, essential oil, proteins, and panaxatriol. The antimicrobial activity of ginseng species has been demonstrated through various mechanisms, including inhibition of microbial motility, inhibition of quorum sensing capacity, inhibition of biofilm formation and destruction of manufactured biofilms, leakage of cell components due to disruption of the membrane lipid layer, enhancement of immunity and alleviation of microbial infections and their complications such as inflammation and DNA damage, and inhibition of antibiotic efflux. Soyuçok et al.[30] reported that the potent antimicrobial activity of ginseng extract was demonstrated against biofilm-forming pathogenic bacteria, including *S. aureus*, *S. typhimurium*, and *L. monocytogenes*. Ginseng extract was found to be able to inhibit *S. aureus*, *S. typhimurium*, and *L. monocytogenes* at different MIC values, of 90, 70, and 40 mg/ml, respectively. The present results indicate that UV-C exposure enhances the antimicrobial activity of GEO by altering its chemical composition, with maximal effects observed after 60 min of exposure. UV-C irradiation has been reported to improve the biological and antibacterial properties of natural oils by modifying their chemical makeup and increasing their effectiveness against target microorganisms, in addition to providing non-thermal sterilization through microbial DNA damage. When combined with essential oils, UV-C treatment may reduce the required concentrations of both the oils and UV intensity, thereby enhancing microbial inactivation while minimizing potential adverse effects on oil quality and product integrity[19].

Determination of mics

GOE demonstrated effective antimicrobial activity with varying MIC values (µg/mL) at different UV-C exposure times (Fig. 3). *B. subtilis* was inhibited at 125, 62.5, and 31.25 µg/mL at 0 min, 30 min, and 60 min, respectively, while *S. aureus* was inhibited at 125, 125, and 62.5 µg/mL over the same intervals, indicating that *B. subtilis* was more sensitive to GOE among Gram-positive bacteria. For Gram-negative bacteria, *K. pneumoniae* was inhibited at 250, 125, and 31.25 µg/mL, and *S. typhi* at 125, 62.5, and 15.62 µg/mL at 0 min, 30 min, and 60 min, respectively. Among Gram-negative bacteria, *S. typhi* was more sensitive to GOE than *K. pneumoniae*. *C. albicans* was the most sensitive pathogen overall, with inhibition observed at 62.5, 15.62, and 15.62 µg/mL at 0 min, 30 min, and 60 min, respectively. Overall, GOE exposed to UV-C for 60 min exhibited the lowest MICs against all tested pathogens, followed by GOE at 30 min and 0 min. Soyoung et al.[31] reported that methanolic and

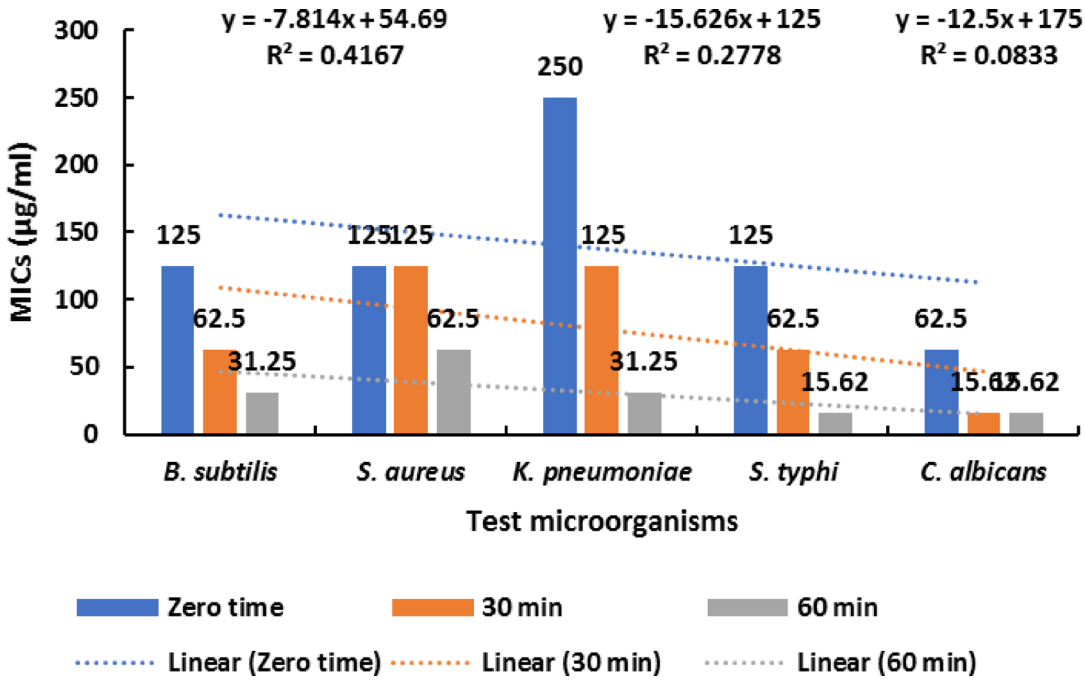

Fig. 3. MICs of GOE at different time intervals against different pathogens (There is a dramatic reduction $P \leq 0.05$ in MIC levels via raise of exposing time to UV-C).

ethanolic ginseng extracts exhibited different MIC values against *B. cereus* and *S. aureus* over 1–16 h at varying temperatures. The ethanolic extract showed the highest antimicrobial activity at 100 °C, with a MIC of 6.25 mg/ml. The methanolic extract of ginseng showed MIC values of 12.5, 25, 12.5, and 100 mg/ml against *S. aureus* at 60, 80, 100, and 120 °C, respectively. Ethanolic extracts showed no difference in antimicrobial activities against *S. aureus* regardless of temperature, except for a lower MICs of ginseng extract at 120 °C. Antimicrobial activity against *B. cereus* increased with the heat treatment period. The antimicrobial activities of ginseng extract at 100 °C for 16 h were four and eight times higher for methanolic and ethanolic extracts, respectively, compared to the corresponding unheated ginseng extracts, both of which had a MIC concentration of 1.56 mg/ml. For *S. aureus*, the methanolic and ethanolic ginseng extracts heated at 100 °C for 2 h exhibited a MIC of 6.25 mg/mL, which was eight times higher than that of the corresponding unheated extracts.

Determination of MBCs

GOE at specific concentrations exhibited bactericidal activity, not just growth inhibition, with varying minimum bactericidal concentrations (MBCs, µg/mL) observed at different time intervals (Fig. 4). *B. subtilis* was killed at 250, 125, and 62.5 µg/ml for 0-time, 30 min, and 60 min, respectively. *S. aureus* was killed at 125, 125, and 62.5 µg/ml for 0-time, 30 min, and 60 min, respectively. In Gram-positive bacteria, MBC values were found to be similar, except at 0-time, *B. subtilis* was more resistant than *S. aureus*, with the former being killed at 250 µg/ml compared to the latter being killed at 125 µg/ml. *K. pneumoniae* was killed at 500, 125, and 62.5 µg/ml for 0-time, 30 min, and 60 min, respectively. *S. typhi* was inhibited at 500, 125, and 31.25 µg/ml for 0-time, 30 min, and 60 min, respectively. In Gram-negative bacteria, MBC values were found to be similar, except at 60 min, *K. pneumoniae* was more resistant than *S. typhi*, with the former being killed at 62.5 µg/ml compared to the latter being killed at 31.25 µg/ml. Among all tested pathogens, *C. albicans* was the most sensitive to GOE, with inhibition observed at 125, 62.5, and 31.25 µg/mL at 0 min, 30 min, and 60 min, respectively. Therefore, GOE at 60 min showed the lowest MIC for inhibition of the tested pathogens, followed by GOE at 30 min, and GOE at 0-time. Campana et al.[31] reported that many essential oils extracted from different plants, including *P. ginseng*, *C. sativa*, *C. carvi*, *C. maritimum*, *C. cyminum*, *C. leylandii*, *C. arizonica*, *F. assafoetida*, *F. gummosa*, *J. communis*, *J. pfitzeriana*, and *P. anisum*, have shown significant antimicrobial activities against pathogenic microbes, including *E. coli*, *L. monocytogenes*, *S. aureus*, *P. fluorescens*, and *C. albicans*. Microemulsions derived from these essential oils (< 50 nm) showed higher stability over 30 days, and exhibited antimicrobial activities with lower MIC and MBC values. The microemulsion of *C. cyminum* showed a MIC two-fold lower (0.312%) than the corresponding essential oil extract (0.625%) and even eight-fold lower against *S. aureus* (0.156 vs. 1.25%). A more pronounced microbicidal effect was observed for the microemulsion of *C. cyminum* with MBCs values eight-fold lower (from 0.312 to 0.625%) than the corresponding essential oil extract (from 2.5 to 5%), and four-fold lower (0.312 vs. 1.25%) only in the cases of *P. fluorescens*. The microemulsion of *P. anisum* showed two-fold lower MIC values (1.25%) with *E. coli*, *L. monocytogenes*, and *S. aureus* compared to the essential oil extract (2.5%), reaching a four-fold lower MIC (0.132%) for *P. fluorescens* and *C. albicans* (MIC in oil extract 1.25%). The MBCs values of the microemulsion of *P. anisum* were 2.5% for most of the examined microorganisms and 1.25% in the case of *P. fluorescens*, in contrast to the free essential oil extract for which MICs values are always greater

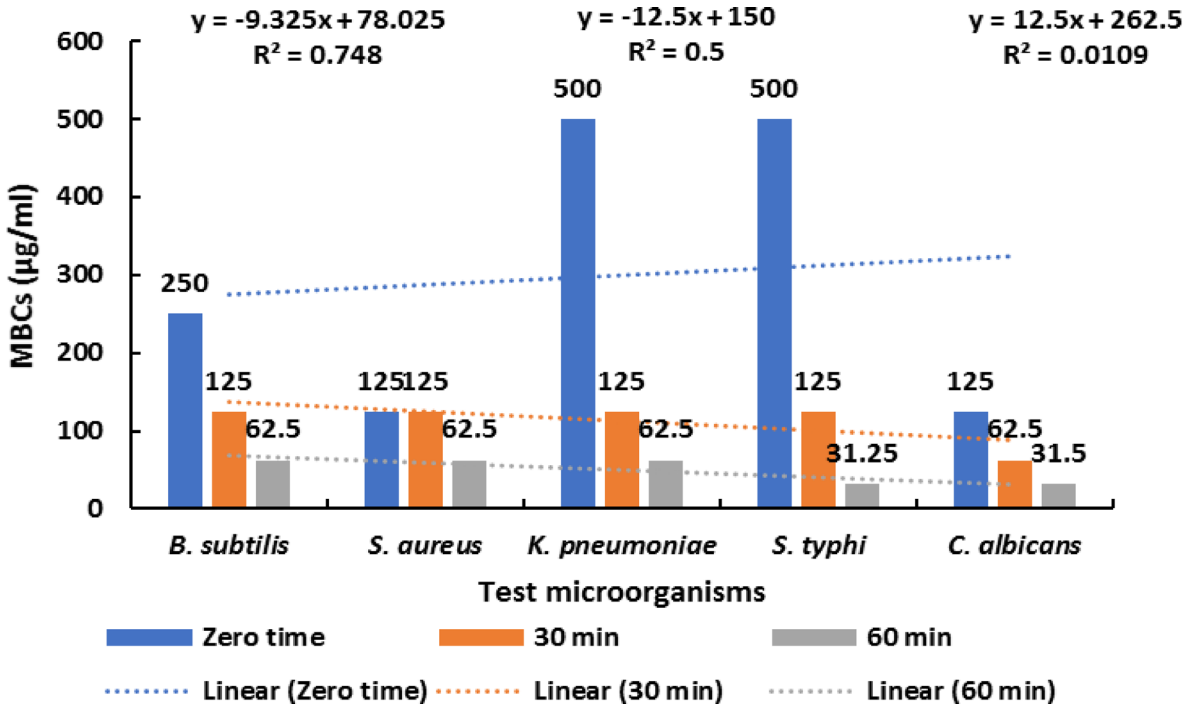

Fig. 4. MBCs of GOE at different periods against different microorganisms (There is a significant reduction $P \leq 0.05$ in MBCs levels via raise of exposing time to UV-C).

than 5%. For the microemulsion of *C. maritimum*, a two-fold lower MIC (1.25%) was observed against *E. coli*, while for *P. fluorescens* and *C. albicans* a four-fold lower MIC (1.25% and 0.312%) was obtained compared to the respective essential oil extract (2.5 and 1.25%). In contrast, no difference was observed for *L. monocytogenes* and *S. aureus* (1.25% for both microemulsion and free essential oil extract). An MBCs value of 2.5% was observed for *E. coli*, *L. monocytogenes*, and *S. aureus* compared to MBCs values greater than or equal to 5% of free essential oil extract, reaching an MBC of 1.25% in the case of *P. fluorescens* and *C. albicans* (four-fold lower than the MBCs). The MBCs/MICs ratio showed, in most cases, the bactericidal effect (MBCs/MICs less than or equal to 4) of the examined microemulsions, except for the microemulsion of *P. anisum* against *C. albicans* (MBCs/MICs greater than 4). MICs and MBCs of natural oils can be considerably decreased by UV-C irradiation, which means that lower amounts of the oil are more efficient at inhibiting or killing microorganisms. This increase in antimicrobial activity is frequently associated with modifications to the oil's chemical makeup, as UV-C exposure can create new compounds and change those that already exist, potentially making them more effective against a range of microbes[32,33].

In vitro assay of anti-inflammatory activity

Different concentrations of GOE exhibited anti-inflammatory activity compared to SDS as a standard at various time intervals. SDS caused 100% hemolysis of red blood cells (RBCs) for all pathogens, whereas GOE at concentrations of 25%, 50%, and 75% showed reduced hemolysis, with lower hemolysis rates indicating higher anti-inflammatory activity. For *B. subtilis*, hemolysis was reduced to 36.5%, 16.3%, and 6.7% at 0 min with 25%, 50%, and 75% GOE, respectively (Figs. 5A and 6A); to 6.7%, 5.9%, and 4.3% at 30 min (Figs. 5A and 6B); and to 5.7%, 4.9%, and 3.6% at 60 min (Figs. 5A and 6C). Therefore, 75% GOE at 60 min was found to have the highest anti-inflammatory activity, followed by 50% and 25%. The same results were obtained at 30 min and 0-time, with the former being more effective than the latter. The inflammation caused by *S. aureus* infection was reduced by 25%, 50%, and 75% with GOE to 68.5%, 41%, and 9.6%, respectively, at 0-time (Figs. 5B and 6D), while it was reduced by 25%, 50%, and 75% with GOE to 55.2%, 12.4%, and 5.5%, respectively, at 30 min (Figs. 5B and 6E), and it was reduced by 25%, 50%, and 75% with GOE to 13.3%, 6.3%, and 3.2%, respectively, at 60 min (Figs. 5B.6 F). Therefore, 75% GOE at 60 min was found to have the highest anti-inflammatory activity, followed by 50% and 25%. The same results were obtained at 30 min and 0-time, with the former being more effective than the latter. The inflammation caused by *K. pneumoniae* infection was reduced by 25%, 50%, and 75% with GOE to 27.1%, 9.7%, and 5.8%, respectively, at 0-time (Figs. 5C and 6G), while it was reduced by 25%, 50%, and 75% with GOE to 14.7%, 6%, and 4.2%, respectively, at 30 min (Figs. 5C and 6H), and it was reduced by 25%, 50%, and 75% with GOE to 7.7%, 3.9%, and 2.1%, respectively, at 60 min (Figs. 5C.6I). Therefore, 75% GOE at 60 min was found to have the highest anti-inflammatory activity, followed by 50% and 25%. The same results were obtained at 30 min and 0-time, with the former being more effective than the latter. For *S. typhi*, inflammation was reduced by GOE in a concentration- and time-dependent manner. At 0 min, hemolysis was 63.6%, 24.1%, and 8.1% for 25%, 50%, and 75% GOE, respectively (Figs. 5D and 6J); at 30 min, it decreased to 18.4%, 10.8%, and 5.1% (Figs. 5D and 6K); and at 60 min, it further decreased to 11.1%, 6.3%, and 2.9% (Figs. 5D and 6L). Overall, 75% GOE at 60 min

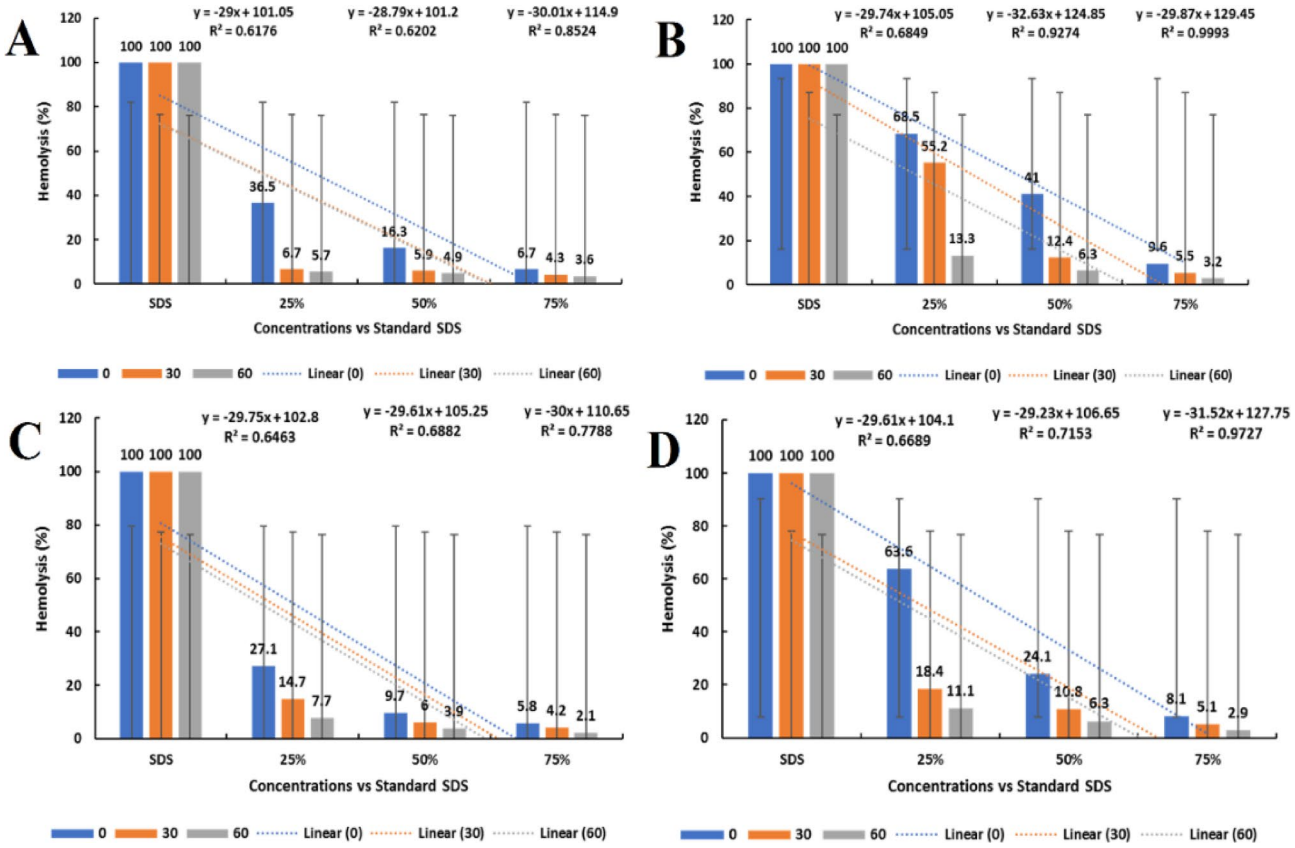

Fig. 5. Anti-inflammatory activity of different concentrations of GOE at different time intervals against: (A) *B. subtilis*, (B) *S. aureus*, (C) *K. pneumoniae*, (D) *S. typhi*. (There is a notable reduction in hemolysis inhibition percentage via raise of exposing time to UV-C upon using various levels of MIC where $P \leq 0.05$; Data are represented as means ± SD).

exhibited the highest anti-inflammatory activity, followed by 50% and 25%, with similar trends observed at 30 min and 0 min, the former being more effective than the latter. Lee et al.[34] reported that *P. ginseng* was used as an important anti-inflammatory. Ginseng extract has been shown to inhibit nitric oxide formation and mRNA activation of inducible nitric oxide synthase in mouse macrophages, but it did not inhibit cyclooxygenase-2 production. The expression pattern of mRNA of tumor necrosis factor alpha and IL-6 was also reduced by ginseng extract. Furthermore, ginseng extract exhibited anti-inflammatory effects by downregulating c-Jun NH_2-terminal kinase phosphorylation, extracellular signal-regulated kinase phosphorylation, and nuclear factor kappa B signaling pathway. The anti-inflammatory regulatory activity of ginseng extract could be stimulated by nitric oxide synthase and inhibition of nitric oxide formation mediated by regulation of nuclear factor kappa B and p38/JNK MAPK pathways. Angeloni et al.[35] reported that *P. ginseng* has been used as a medicinal plant in many countries, especially in East Asia, due to its therapeutic properties, including antioxidant, anti-inflammatory, and anticancer properties. Macrophages activated by lipopolysaccharides (the outer membrane material of Gram-negative bacteria) stimulate the formation and release of components involved in triggering inflammation, including cytokines, nitric oxide, and pro-inflammatory enzymes. Accumulating evidence suggests that nitric oxide is involved as an initiator of inflammation. Nitric oxide performs essential functions as a signaling molecule in many physiological processes, and high concentrations of nitric oxide formed by the enzyme nitric oxide synthase can lead to inflammation. The current findings revealed that GEO exposed to UV-C increases its anti-inflammatory effects by changing the chemical makeup of the resulting GEO, with the maximum effect occurring after 60 min of UV-C exposure. Certain natural oils, like aloe vera, can have their anti-inflammatory qualities strengthened by UV-C irradiation since it raises their levels of active ingredients. Research indicates that extending an oil's UV-C exposure duration yields a stronger anti-inflammatory impact. Technology that can boost bioactive molecules is used in this method, which could have positive benefits on UV-damage prevention[19].

Microtiter plate assay for biofilm quantification

Different concentrations of GOE exhibited anti-biofilm activity against all tested pathogens compared to blank and control at different time intervals. The blank and control with all pathogens could not show anti-biofilm activity, while different concentrations (25, 50, 75%) with all pathogens showed different anti-biofilm activities, where lower anti-biofilm activity indicated less control of antibacterial resistance. The anti-biofilm activity

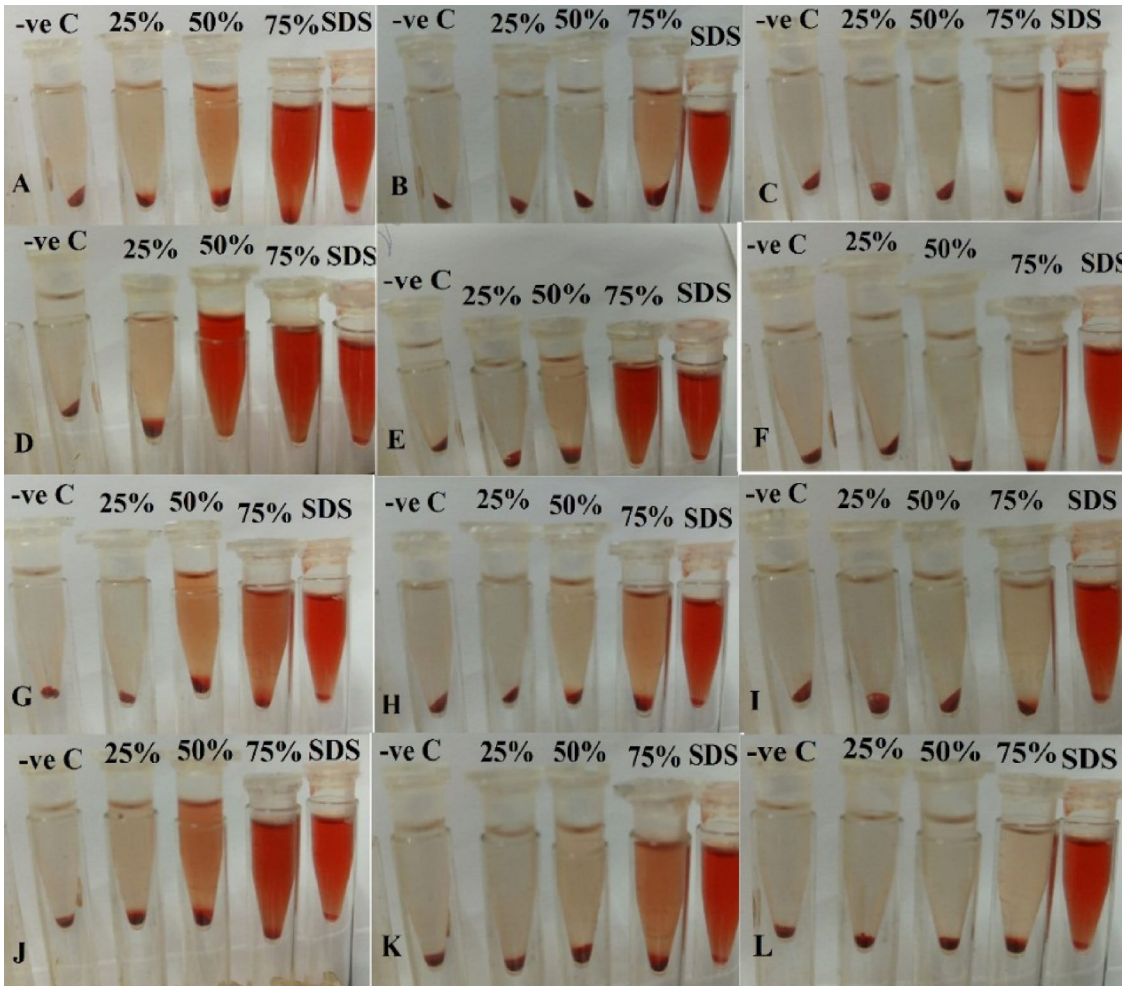

Fig. 6. Anti-inflammatory activity of different concentrations of GOE against: *B. subtilis* at (A) 0-time, (B) 30 min, (C) 60 min, *S. aureus* at (D) 0-time, (E) 30 min, (F) 60 min, *K. pneumoniae* at (G) 0-time, (H) 30 min, (I) 60 min, *S. typhi* at (J) 0-time, (K) 30 min, and (L) 60 min.

against *B. subtilis* was reduced by 25%, 50%, and 75% with GOE to 82.85%, 65.72%, and 21.18%, respectively, at 0-time, while it was reduced by 25%, 50%, and 75% with GOE to 86.71%, 74.66%, and 29.97%, respectively, at 30 min, and it was reduced by 25%, 50%, and 75% with GOE to 92.84%, 77.85%, and 72.98%, respectively, at 60 min (Figs. 7A and 8A). Therefore, 25% GOE at 60 min was found to have the highest anti-biofilm activity, followed by 50% and 75%. The same results were obtained at 30 min and 0-time, with the former being more effective than the latter. The anti-biofilm activity against *S. aureus* was reduced by 25%, 50%, and 75% with GOE to 74.9%, 52.19%, and 20.26%, respectively, at 0-time, while it was reduced by 25%, 50%, and 75% with GOE to 84.66%, 62.55%, and 40.8%, respectively, at 30 min, and it was reduced by 25%, 50%, and 75% with GOE to 92.24%, 79.72%, and 71.58%, respectively, at 60 min (Figs. 7B and 8B). Therefore, 25% GOE at 60 min was found to have the highest anti-biofilm activity, followed by 50% and 75%. The same results were obtained at 30 min and 0-time, with the former being more effective than the latter. The anti-biofilm activity against *K. pneumoniae* was reduced by 25%, 50%, and 75% with GOE to 76.73%, 43.58%, and 14.39%, respectively, at 0-time, while it was reduced by 25%, 50%, and 75% with GOE to 85.1%, 66.82%, and 34.7%, respectively, at 30 min, and it was reduced by 25%, 50%, and 75% with GOE to 92.54%, 87.91%, and 49.72%, respectively, at 60 min (Figs. 7C and 8C). Therefore, 25% GOE at 60 min was found to have the highest anti-biofilm activity, followed by 50% and 75%. The same results were obtained at 30 min and 0-time, with the former being more effective than the latter. The anti-biofilm activity against *S. typhi* was reduced by 25%, 50%, and 75% with GOE to 77.52%, 59.22%, and 13.54%, respectively, at 0-time, while it was reduced by 25%, 50%, and 75% with GOE to 87.99%, 75.67%, and 50.13%, respectively, at 30 min, and it was reduced by 25%, 50%, and 75% with GOE to 93.82%, 81.5%, and 65.05%, respectively, at 60 min (Figs. 7D and 8D). Therefore, 25% GOE at 60 min was found to have the highest anti-biofilm activity, followed by 50% and 75%.

The same results were obtained at 30 min and 0-time, with the former being more effective than the latter. Natural oils, such as clove and cinnamon oil, exposed to UV-C radiation hinder bacterial adhesion and break the extracellular matrix of biofilms, while inactivates germs by causing DNA damage. These two substances work in concert to combat biofilms. This strategy offers a non-thermal, non-toxic choice for biofilm reduction in a

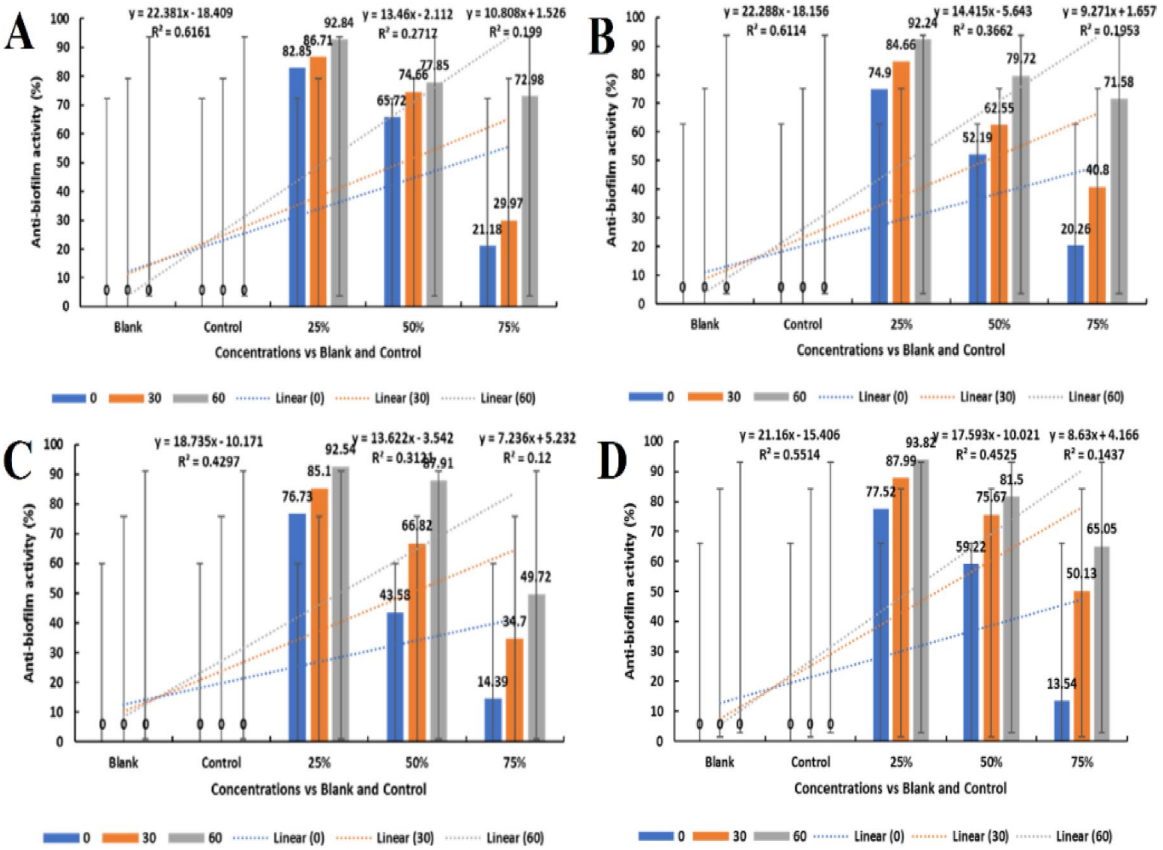

Fig. 7. Anti-biofilm activity of different concentrations of GOE at different time intervals against: (A) *B. subtilis*, (B) *S. aureus*, (C) *K. pneumoniae*, and (D) *S. typhi*. (There is a notable reduction in antibiofilm via raise of exposing time to UV-C upon using various levels of MBC where $P \leq 0.05$ Upon using 75% MBCs; $P > 0.05$ upon using 50, 25% of MBCs; Data are represented as means ± SD).

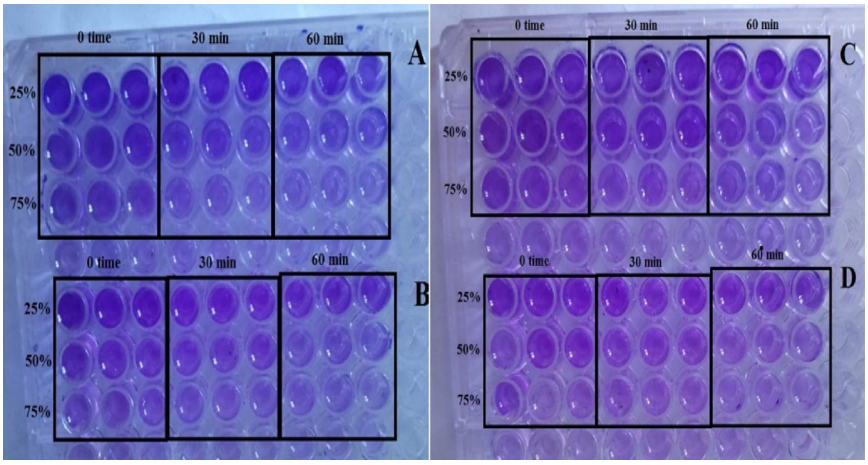

Fig. 8. Anti-biofilm activity of different concentrations of GOE against: (A) *B. subtilis* at 0-time, 30 min, 60 min, (B) *S. aureus* at 0-time, 30 min, 60 min, (C) *K. pneumoniae* at 0-time, 30 min, 60 min, (D) *S. typhi* at 0-time, 30 min, and 60 min.

variety of applications, with increased efficacy[19]. Extracts of *P. ginseng* and *S. officinale* demonstrated antibacterial activity against *P. gingivalis*, inhibiting the production of quorum sensing molecules and preventing new biofilm formation. Both extracts exhibited a synergistic effect with the antibiotic metronidazole, significantly enhancing its antibacterial efficacy[15]. In terms of biofilm formation and quorum sensing, these findings highlight the potential of plant-derived compounds to develop more effective strategies for managing periodontal bacterial

infections. However, future studies should aim to identify the precise bioactive substances responsible for these antibacterial activities as well as evaluating the efficacy and safety of these extracts in human clinical trials[36,37]. Overall, both *P. ginseng* and *S. officinale* show strong antibacterial activity against *P. gingivalis*, including inhibition of bacterial growth and disruption of established biofilms[38].

GS-MS analysis

GOE-0-time was analyzed using GC-MS and found to contain 24 compounds at different retention times (RTs), area ratios, and probability ratios (Table 1). As shown in (Fig. 9A), 7,11,15-Trimethyl-3-methylene-hexadeca-1,6,10,14-tetraene ($C_{20}H_{32}$, 272 g/mol) appeared as peak 1 with a RT of 46.21 min and an area of 0.28%. Hexadecanoic acid, methyl ester ($C_{17}H_{34}O_2$, 270 g/mol) appeared as peak 2 with a RT of 46.46 min and an area of 0.59%. 9,12-Octadecadienoyl chloride ($C_{18}H_{31}ClO$, 298 g/mol) appeared as peak 3 with a RT of 63.45 min and an area of 0.88%. Palmitoleic acid ($C_{16}H_{30}O_2$, 254 g/mol) appeared as peak 4 with a RT of 47.80 min and an area of 0.18%. n-Hexadecanoic acid ($C_{16}H_{32}O_2$, 256 g/mol) appeared as peaks 5 with a RT of 48.95 min and an area of 4.30%. 9,12-Octadecadienoic acid (Z, Z)-, methyl ester ($C_{19}H_{34}O_2$, 294 g/mol) appeared as peak 6 with a RT of 51.77 min and an area of 4.95%. Heptadecanoic acid, 16-methyl-, methyl ester ($C_{19}H_{38}O_2$, 298 g/mol) appeared as peak 7 with a RT of 52.65 min and an area of 0.41%. Ethyl (9Z,12Z)-9,12-octadecadienoate ($C_{20}H_{36}O_2$, 308 g/mol) appeared as peak 8 with a RT of 53.49 min and an area of 1.84%. 9-Octadecenoic acid ethyl ester ($C_{20}H_{38}O_2$, 310 g/mol) appeared as peak 9 with a RT of 53.84 min and an area of 7.14%. 9,12-Octadecadienoic acid ($C_{18}H_{32}O_2$, 280 g/mol) appeared as peak 10 with a RT of 54.01 min and an area of 0.46%. 9-Octadecenoic acid ($C_{18}H_{34}O_2$, 282 g/mol) appeared as peak 11 with a RT of 54.86 min and an area of 1.17%. Oleic acid ($C_{18}H_{34}O_2$, 282 g/mol) appeared as peak 12 with a RT of 56.57 min and an area of 1.06%. trans-13-Octadecenoic acid ($C_{18}H_{34}O_2$, 282 g/mol) appeared as peak 13 with a RT of 55.45 min and an area of 7.72%. 9,12-Octadecadienoic acid (Z, Z)-, 2-hydroxy-1-(hydroxymethyl) ethyl ester ($C_{21}H_{38}O_4$, 354 g/mol) appeared as peak 14 with a RT of 62.12 min and an area of 3.41%. 9-Octadecenoic acid (Z)-, 2,3-dihydroxypropyl ester ($C_{21}H_{40}O_4$, 356 g/mol) appeared as peak 15 with a RT of 62.39 min and an area of 7.09%. 13-Docosenamide ($C_{22}H_{43}NO$, 337 g/mol) appeared as peak 16 with a RT of 71.58 min and an area of 1.22%. Arg-Leu-Lys ($C_{18}H_{37}N_7O_4$, 415 g/mol) appeared as peak 17 with a RT of 77.92 min and an area of 2.27%. (+)-Sesamin ($C_{20}H_{18}O_6$, 354 g/mol) appeared as peak 18 with a RT of 79.59 min and an area of 23.62%. 5-(1R,3aR,4 S,6aR)-4-(Benzo[d]$^{(1,3)}$ dioxol-5-yl) hexahydrofuro [3, 4-c] furan-1-yl) oxy) benzo [d]$^{(1,3)}$ dioxol ($C_{20}H_{18}O_7$, 370 g/mol) appeared as peak 19 with a RT of 80.65 min and an area of 13.80%. 5,10-Secocholest-1(10)-EN-3,5-dione ($C_{27}H_{44}O_2$, 400 g/mol) appeared as peak 20 with a RT of 81.30 min and an area of 0.6%. Stigmasterol ($C_{29}H_{48}O$, 412 g/mol) appeared as peak 21 with a RT of 81.93 min and an area of 0.42%. Stigmast-5-EN-3-OL, (3á,24 S) ($C_{29}H_{50}O$, 414 g/mol) appeared as peak 22 with a RT of 83.21 min

Peak	RT (min)	Area (%)	Compound*	Probability (%)	Formula	MW (g/mol)
1	46.21	0.28	7,11,15-Trimethyl-3-methylene-hexadeca-1,6,10,14-tetraene	44.73	$C_{20}H_{32}$	272
2	46.46	0.59	Hexadecanoic acid, methyl ester	50.81	$C_{17}H_{34}O_2$	270
3	63.45	0.88	9,12-Octadecadienoyl chloride	26.11	$C_{18}H_{31}ClO$	298
4	47.80	0.18	Palmitoleic acid	14.63	$C_{16}H_{30}O_2$	254
5	48.95	4.30	n-Hexadecanoic acid	73.61	$C_{16}H_{32}O_2$	256
6	51.77	4.95	9,12-Octadecadienoic acid (Z, Z)-, methyl ester	12.57	$C_{19}H_{34}O_2$	294
7	52.65	0.41	Heptadecanoic acid, 16-methyl-, methyl ester	20.45	$C_{19}H_{38}O_2$	298
8	53.49	1.84	Ethyl (9Z,12Z)-9,12-octadecadienoate	10.60	$C_{20}H_{36}O_2$	308
9	53.84	7.14	9-Octadecenoic acid ethyl ester	12.33	$C_{20}H_{38}O_2$	310
10	54.01	0.46	9,12-Octadecadienoic acid	36.11	$C_{18}H_{32}O_2$	280
11	54.86	1.17	9-Octadecenoic acid	44.05	$C_{18}H_{34}O_2$	282
12	56.57	1.06	Oleic acid	30.72	$C_{18}H_{34}O_2$	282
13	55.45	7.72	trans-13-Octadecenoic acid	21.09	$C_{18}H_{34}O_2$	282
14	62.12	3.41	9,12-Octadecadienoic acid (Z, Z)-, 2-hydroxy-1-(hydroxymethyl)ethyl ester	33.22	$C_{21}H_{38}O_4$	354
15	62.39	7.09	9-Octadecenoic acid (Z)-, 2,3-dihydroxypropyl ester	13.83	$C_{21}H_{40}O_4$	356
16	71.58	1.22	13-Docosenamide	38.03	$C_{22}H_{43}NO$	337
17	77.92	2.27	Arg-Leu-Lys	20.04	$C_{18}H_{37}N_7O_4$	415
18	79.59	23.62	(+)-Sesamin	59.60	$C_{20}H_{18}O_6$	354
19	80.65	13.80	5-(1R,3aR,4 S,6aR)-4-(Benzo[d] (1,3) dioxol-5-yl) hexahydrofuro [3, 4-c] furan-1-yl) oxy) benzo [d] (1,3) dioxol	90.28	$C_{20}H_{18}O_7$	370
20	81.30	0.60	5,10-Secocholest-1(10)-EN-3,5-dione	15.46	$C_{27}H_{44}O_2$	400
21	81.93	0.42	Stigmasterol	24.33	$C_{29}H_{48}O$	412
22	83.21	2.63	Stigmast-5-EN-3-OL, (3á,24 S)	51.17	$C_{29}H_{50}O$	414
23	83.47	0.34	Ergosta-5,24(28)-dien-3-OL, (3á)	35.80	$C_{28}H_{46}O$	398
24	85.96	0.96	Stigmast-4-EN-3-ONE	30.98	$C_{29}H_{48}O$	412

Table 1. GC-MS analysis of unexposed GOE to UV-C (time 0 min).

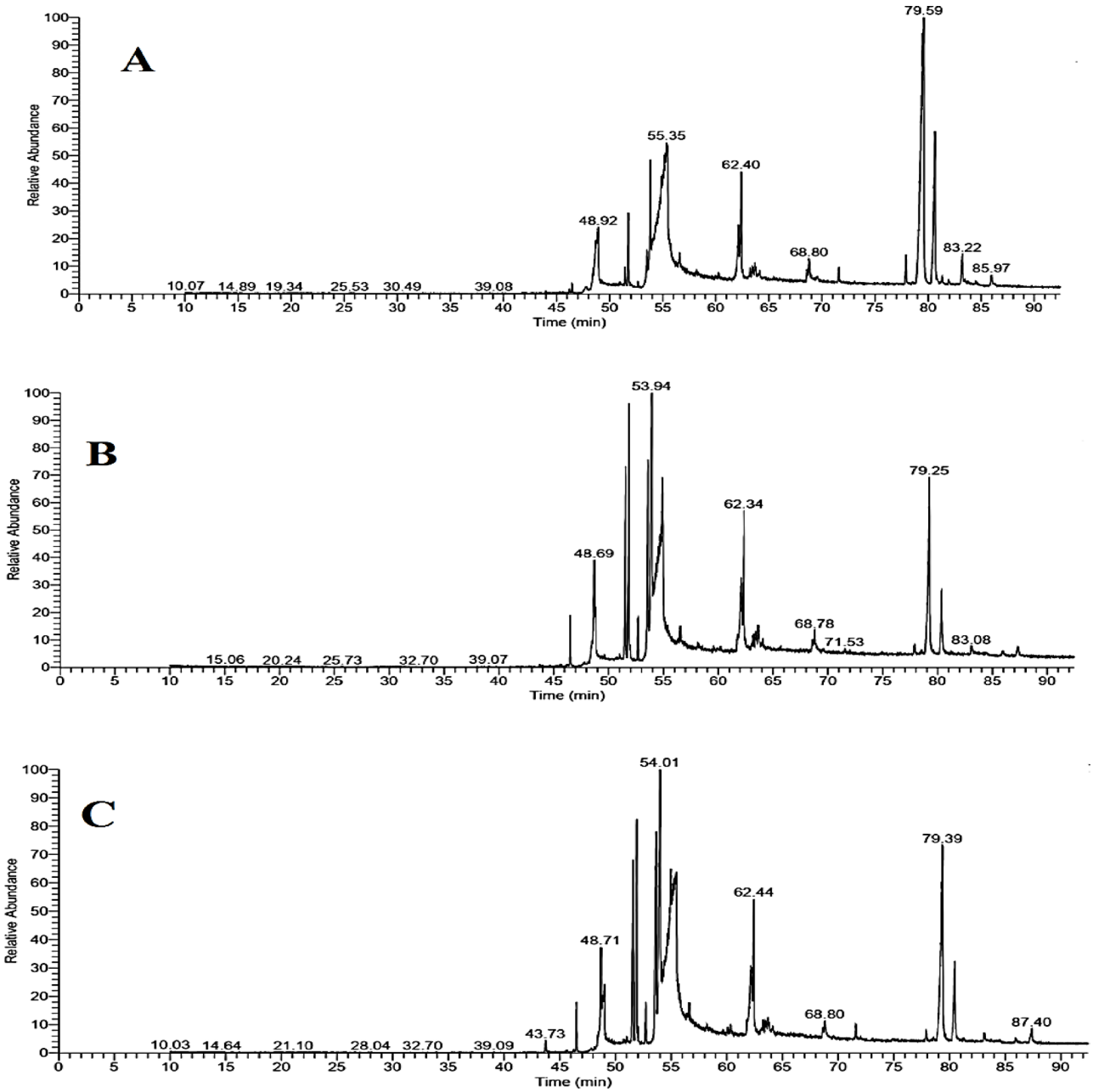

Fig. 9. GC-MS analysis of GOE at: (A) 0-time, (B) 30 min, (C) 60 min.

and an area of 2.63%. Ergosta-5,24(28)-dien-3-OL, (3á) ($C_{28}H_{46}O$, 398 g/mol) appeared as peak 23 with a RT of 83.47 min and an area of 0.34%. Stigmast-4-EN-3-ONE ($C_{29}H_{48}O$, 412 g/mol) appeared as peak 24 with a RT of 85.96 min and an area of 0.96%.

GOE-30-min was analyzed using GC-MS and found to contain 24 compounds at different RTs, area ratios, and probability ratios (Table 2). As shown in (Fig. 9B), Hexadecanoic acid, methyl ester ($C_{17}H_{34}O_2$, 270 g/mol) appeared as peak 1 with a RT of 46.50 min and an area of 2.5%. 9-Octadecenoic acid ($C_{18}H_{34}O_2$, 282 g/mol) appeared as peak 2 with a RT of 54.92 min and an area of 7.56%. Hexadecanoic acid, ethyl ester ($C_{18}H_{36}O_2$, 284 g/mol) appeared as peak 3 with a RT of 48.68 min and an area of 4.78%. n-Hexadecanoic acid ($C_{16}H_{32}O_2$, 256 g/mol) appeared as peak 4 with a RT of 48.83 min and an area of 2.29%. Oleic acid ($C_{18}H_{34}O_2$, 282 g/mol) appeared as peaks 5 with a RT of 56.55 min and an area of 0.87%. 9,12-Octadecadienoic acid (Z, Z)-, methyl ester ($C_{19}H_{34}O_2$, 294 g/mol) appeared as peak 6 with a RT of 51.84 min and an area of 10.26%. 9-Octadecenoic acid, methyl ester ($C_{19}H_{36}O_2$, 296 g/mol) appeared as peak 7 with a RT of 51.87 min and an area of 14.08%. Methyl stearate ($C_{19}H_{38}O_2$, 298 g/mol) appeared as peak 8 with a RT of 52.69 min and an area of 1.89%. Ethyl (9Z,12Z)-9,12-octadecadienoate ($C_{20}H_{36}O_2$, 308 g/mol) appeared as peak 9 with a RT of 53.59 min and an area of 9.9%. Ethyl oleate ($C_{20}H_{38}O_2$, 310 g/mol) appeared as peak 10 with a RT of 53.93 min and an area of 13.17%. 9,12-Octadecadienoic acid ($C_{18}H_{32}O_2$, 280 g/mol) appeared as peak 11 with a RT of 68.56 min and an area of

Peak	RT (min)	Area (%)	Compound*	Probability (%)	Formula	MW (g/mol)
1	46.50	2.50	Hexadecanoic acid, methyl ester	67.74	$C_{17}H_{34}O_2$	270
2	54.92	7.56	9-Octadecenoic acid	18.15	$C_{18}H_{34}O_2$	282
3	48.68	4.78	Hexadecanoic acid, ethyl ester	47.80	$C_{18}H_{36}O_2$	284
4	48.83	2.29	n-Hexadecanoic acid	63.61	$C_{16}H_{32}O_2$	256
5	56.55	0.87	Oleic acid	29.32	$C_{18}H_{34}O_2$	282
6	51.84	10.26	9,12-Octadecadienoic acid (Z, Z)-, methyl ester	11.36	$C_{19}H_{34}O_2$	294
7	51.87	14.08	9-Octadecenoic acid, methyl ester	12.32	$C_{19}H_{36}O_2$	296
8	52.69	1.89	Methyl stearate	33.25	$C_{19}H_{38}O_2$	298
9	53.59	9.90	Ethyl (9Z,12Z)-9,12-octadecadienoate	24.24	$C_{20}H_{36}O_2$	308
10	53.93	13.17	Ethyl oleate	19.44	$C_{20}H_{38}O_2$	310
11	68.56	0.48	9,12-Octadecadienoic acid	6.84	$C_{18}H_{32}O_2$	280
12	68.78	0.84	9,12-Octadecadienoyl chloride	7.59	$C_{18}H_{31}ClO$	298
13	62.09	3.32	9,12-Octadecadienoic acid (Z, Z)-, 2-hydroxy-1-(hydroxymethyl)ethyl ester	8.32	$C_{21}H_{38}O_4$	354
14	62.35	5.75	Oleic acid, 3-hydroxypropyl ester	14.29	$C_{21}H_{40}O_3$	340
15	68.78	0.84	trans-13-Octadecenoic acid	5.50	$C_{18}H_{34}O_2$	282
16	63.64	1.02	9-Octadecenoic acid (Z)-, oxiranyl methyl ester	19.16	$C_{21}H_{38}O_3$	338
17	68.78	0.84	2-Hydroxy-3-[(9E)-9-octadecenoyloxy] propyl (9E)-9-octadecenoate	7.00	$C_{39}H_{72}O_5$	620
18	71.53	0.24	17-Octadecynoic acid	4.97	$C_{18}H_{32}O_2$	280
19	77.88	0.48	(5à,6à)-4,5-Epoxy-17-methyl-3-phthalimidomorphinan-6-OL	48.39	$C_{25}H_{24}N_2O_4$	416
20	85.93	0.27	9-Octadecenoic acid, 1,2,3-propanetriyl ester	5.08	$C_{57}H_{104}O_6$	884
21	79.26	9.75	(+)-Sesamin	59.24	$C_{20}H_{18}O_6$	354
22	80.38	3.17	5-(1R,3aR,4 S,6aR)-4-(Benzo[d] (1,3) dioxol-5-yl) hexahydrofuro [3, 4-c] furan-1-yl) oxy) benzo [d] (1,3) dioxol	92.18	$C_{20}H_{18}O_7$	370
23	83.09	0.47	Stigmast-5-EN-3-OL, (3á,24 S)	46.10	$C_{29}H_{50}O$	414
24	87.35	0.70	cis-Vaccenic acid	6.71	$C_{18}H_{34}O_2$	282

Table 2. GC-MS analysis of exposed GOE to UV-C for 30 min.

0.48%. 9,12-Octadecadienoyl chloride ($C_{18}H_{31}ClO$, 298 g/mol) appeared as peak 12 with a RT of 68.78 min and an area of 0.84%. 9,12-Octadecadienoic acid (Z, Z)-, 2-hydroxy-1-(hydroxymethyl) ethyl ester ($C_{21}H_{38}O_4$, 354 g/mol) appeared as peak 13 with a RT of 62.09 min and an area of 3.32%. Oleic acid, 3-hydroxypropyl ester ($C_{21}H_{40}O_3$, 340 g/mol) appeared as peak 14 with a RT of 62.35 min and an area of 5.75%. trans-13-Octadecenoic acid ($C_{18}H_{34}O_2$, 282 g/mol) appeared as peak 15 with a RT of 68.78 min and an area of 0.84%. 9-Octadecenoic acid (Z)-, oxiranyl methyl ester ($C_{21}H_{38}O_3$, 338 g/mol) appeared as peak 16 with a RT of 63.64 min and an area of 1.02%. 2-Hydroxy-3-[(9E)-9-octadecenoyloxy] propyl (9E)-9-octadecenoate ($C_{39}H_{72}O_5$, 620 g/mol) appeared as peak 17 with a RT of 68.78 min and an area of 0.84%. 17-Octadecynoic acid ($C_{18}H_{32}O_2$, 280 g/mol) appeared as peak 18 with a RT of 71.53 min and an area of 0.24%. (5à,6à)-4,5-Epoxy-17-methyl-3-phthalimidomorphinan-6-OL ($C_{25}H_{24}N_2O_4$, 416 g/mol) appeared as peak 19 with a RT of 77.88 min and an area of 0.48%. 9-Octadecenoic acid, 1,2,3-propanetriyl ester ($C_{57}H_{104}O_6$, 884 g/mol) appeared as peak 20 with a RT of 85.93 min and an area of 0.27%. (+)-Sesamin ($C_{20}H_{18}O_6$, 354 g/mol) appeared as peak 21 with a RT of 79.26 min and an area of 9.75%. 5-(1R,3aR,4 S,6aR)-4-(Benzo[d]$^{(1,3)}$ dioxol-5-yl) hexahydrofuro [3, 4-c] furan-1-yl) oxy) benzo [d]$^{(1,3)}$ dioxol ($C_{20}H_{18}O_7$, 370 g/mol) appeared as peak 22 with a RT of 80.38 min and an area of 3.17%. Stigmast-5-EN-3-OL, (3á,24 S) ($C_{29}H_{50}O$, 414 g/mol) appeared as peak 23 with a RT of 83.09 min and an area of 0.47%. cis-Vaccenic acid ($C_{18}H_{34}O_2$, 282 g/mol) appeared as peak 24 with a RT of 87.35 min and an area of 0.7%.

GOE-60-min was analyzed using GC-MS and found to contain 29 compounds at different RTs, area ratios, and probability ratios (Table 3). As shown in (Fig. 9C), 1,2-Benzenedicarboxylic acid, bis (2-methylpropyl) ester ($C_{16}H_{22}O_4$, 278 g/mol) appeared as peak 1 with a RT of 43.73 min and an area of 0.53%. 7,11,15-Trimethyl-3-methylene-hexadeca-1,6,10,14-tetraene ($C_{20}H_{32}$, 272 g/mol) appeared as peak 2 with a RT of 46.24 min and an area of 0.1%. Hexadecanoic acid, methyl ester ($C_{17}H_{34}O_2$, 270 g/mol) appeared as peak 3 with a RT of 46.52 min and an area of 2.04%. 9,17-Octadecadienal ($C_{18}H_{32}O$, 264 g/mol) appeared as peak 4 with a RT of 48.12 min and an area of 0.13%. 9-Octadecenoic acid ($C_{18}H_{34}O_2$, 282 g/mol) appeared as peaks 5 with a RT of 55.48 min and an area of 13.52%. Hexadecanoic acid, ethyl ester ($C_{18}H_{36}O_2$, 284 g/mol) appeared as peak 6 with a RT of 48.70 min and an area of 3.04%. n-Hexadecanoic acid ($C_{16}H_{32}O_2$, 256 g/mol) appeared as peak 7 with a RT of 49.03 min and an area of 3.0%. Oleic acid ($C_{18}H_{34}O_2$, 282 g/mol) appeared as peak 8 with a RT of 56.62 min and an area of 0.78%. 9,12-Octadecadienoic acid (Z, Z)-, methyl ester ($C_{19}H_{34}O_2$, 294 g/mol) appeared as peak 9 with a RT of 51.58 min and an area of 8.68%. 9-Octadecenoic acid, methyl ester ($C_{19}H_{36}O_2$, 296 g/mol) appeared as peak 10 with a RT of 51.91 min and an area of 10.91%. Methyl stearate ($C_{19}H_{38}O_2$, 298 g/mol) appeared as peak 11 with a RT of 52.72 min and an area of 1.63%. Ethyl (9Z,12Z)-9,12-octadecadienoate ($C_{20}H_{36}O_2$, 308 g/mol) appeared as peak 12 with a RT of 53.65 min and an area of 9.73%. Ethyl oleate ($C_{20}H_{38}O_2$, 310 g/mol) appeared as peak 13 with a RT of 54.01 min and an area of 13.62%. 9,12-Octadecadienoic acid ($C_{18}H_{32}O_2$,

Peak	RT (min)	Area (%)	Compound*	Probability (%)	Formula	MW (g/mol)
1	43.73	0.53	1,2-Benzenedicarboxylic acid, bis (2-methylpropyl) ester	28.12	$C_{16}H_{22}O_4$	278
2	46.24	0.10	7,11,15-Trimethyl-3-methylene-hexadeca-1,6,10,14-tetraene	34.82	$C_{20}H_{32}$	272
3	46.52	2.04	Hexadecanoic acid, methyl ester	68.94	$C_{17}H_{34}O_2$	270
4	48.12	0.13	9,17-Octadecadienal	13.19	$C_{18}H_{32}O$	264
5	55.48	13.52	9-Octadecenoic acid	26.79	$C_{18}H_{34}O_2$	282
6	48.70	3.04	Hexadecanoic acid, ethyl ester	53.44	$C_{18}H_{36}O_2$	284
7	49.03	3.00	n-Hexadecanoic acid	70.32	$C_{16}H_{32}O_2$	256
8	56.62	0.78	Oleic acid	25.25	$C_{18}H_{34}O_2$	282
9	51.58	8.68	9,12-Octadecadienoic acid (Z, Z)-, methyl ester	12.14	$C_{19}H_{34}O_2$	294
10	51.91	10.91	9-Octadecenoic acid, methyl ester	11.87	$C_{19}H_{36}O_2$	296
11	52.72	1.63	Methyl stearate	31.68	$C_{19}H_{38}O_2$	298
12	53.65	9.73	Ethyl (9Z,12Z)-9,12-octadecadienoate	22.74	$C_{20}H_{36}O_2$	308
13	54.01	13.62	Ethyl oleate	18.55	$C_{20}H_{38}O_2$	310
14	54.12	0.53	9,12-Octadecadienoic acid	36.22	$C_{18}H_{32}O_2$	280
15	63.72	0.61	9,12-Octadecadienoyl chloride	8.87	$C_{18}H_{31}ClO$	298
16	55.68	0.22	cis-Vaccenic acid	7.89	$C_{18}H_{34}O_2$	282
17	60.07	0.36	17-Octadecynoic acid	7.50	$C_{18}H_{32}O_2$	280
18	60.35	0.46	9-Octadecenamide	9.78	$C_{18}H_{35}NO$	281
19	62.17	2.84	9,12-Octadecadienoic acid (Z, Z)-, 2-hydroxy-1-(hydroxymethyl) ethyl ester	32.21	$C_{21}H_{38}O_4$	354
20	62.44	4.81	9-Octadecenoic acid (Z)-, 2,3-dihydroxypropyl ester	14.57	$C_{21}H_{40}O_4$	356
21	68.81	0.61	2-Hydroxy-3-[(9E)-9-octadecenoyloxy] propyl (9E)-9-octadecenoate	9.84	$C_{39}H_{72}O_5$	620
22	71.59	0.70	13-Docosenamide	11.14	$C_{22}H_{43}NO$	337
23	77.91	0.45	Arg-Leu-Lys	28.55	$C_{18}H_{37}N_7O_4$	415
24	85.96	0.25	9-Octadecenoic acid, 1,2,3-propanetriyl ester	4.07	$C_{57}H_{104}O_6$	884
25	79.39	8.36	(+)-Sesamin	59.62	$C_{20}H_{18}O_6$	354
26	80.49	3.25	5-(1R,3aR,4 S,6aR)-4-(Benzo[d] (1,3) dioxol-5-yl) hexahydrofuro [3, 4-c] furan-1-yl) oxy) benzo [d] (1,3) dioxol	91.09	$C_{20}H_{18}O_7$	370
27	81.31	0.15	Ethyl iso-allocholate	24.73	$C_{26}H_{44}O_5$	436
28	83.13	0.46	Stigmast-5-EN-3-OL, (3á)	51.29	$C_{29}H_{50}O$	414
29	87.40	1.06	2-Methyl-Z, Z-3,13-octadecadienol	8.34	$C_{19}H_{36}O$	280

Table 3. GC-MS analysis of exposed GOE to UV-C for 60 min.

280 g/mol) appeared as peak 14 with a RT of 54.12 min and an area of 0.53%. 9,12-Octadecadienoyl chloride ($C_{18}H_{31}ClO$, 298 g/mol) appeared as peak 15 with a RT of 63.72 min and an area of 0.61%. cis-Vaccenic acid ($C_{18}H_{34}O_2$, 282 g/mol) appeared as peak 16 with a RT of 55.68 min and an area of 0.22%. 17-Octadecynoic acid ($C_{18}H_{32}O_2$, 280 g/mol) appeared as peak 17 with a RT of 60.07 min and an area of 0.36%. 9-Octadecenamide ($C_{18}H_{35}NO$, 281 g/mol) appeared as peak 18 with a RT of 60.35 min and an area of 0.46%. 9,12-Octadecadienoic acid (Z, Z)-, 2-hydroxy-1-(hydroxymethyl) ethyl ester ($C_{21}H_{38}O_4$, 354 g/mol) appeared as peak 19 with a RT of 62.17 min and an area of 2.84%. 9-Octadecenoic acid (Z)-, 2,3-dihydroxypropyl ester ($C_{21}H_{40}O_4$, 356 g/mol) appeared as peak 20 with a RT of 62.44 min and an area of 4.81%. 2-Hydroxy-3-[(9E)-9-octadecenoyloxy] propyl (9E)-9-octadecenoate ($C_{39}H_{72}O_5$, 620 g/mol) appeared as peak 21 with a RT of 68.81 min and an area of 0.61%. 13-Docosenamide ($C_{22}H_{43}NO$, 337 g/mol) appeared as peak 22 with a RT of 71.59 min and an area of 0.7%. Arg-Leu-Lys ($C_{18}H_{37}N_7O_4$, 415 g/mol) appeared as peak 23 with a RT of 77.91 min and an area of 0.45%. 9-Octadecenoic acid, 1,2,3-propanetriyl ester ($C_{57}H_{104}O_6$, 884 g/mol) appeared as peak 24 with a RT of 85.96 min and an area of 0.25%. (+)-Sesamin ($C_{20}H_{18}O_6$, 354 g/mol) appeared as peak 25 with a RT of 79.39 min and an area of 8.36%. 5-(1R,3aR,4 S,6aR)-4-(Benzo[d]$^{(1,3)}$ dioxol-5-yl) hexahydrofuro [3, 4-c] furan-1-yl) oxy) benzo [d]$^{(1,3)}$ dioxol ($C_{20}H_{18}O_7$, 370 g/mol) appeared as peak 26 with a RT of 80.49 min and an area of 3.25%. Ethyl iso-allocholate ($C_{26}H_{44}O_5$, 436 g/mol) appeared as peak 27 with a RT of 81.31 min and an area of 0.15%. Stigmast-5-EN-3-OL, (3á) ($C_{29}H_{50}O$, 414 g/mol) appeared as peak 28 with a RT of 83.13 min and an area of 0.46%. 2-Methyl-Z, Z-3,13-octadecadienol ($C_{19}H_{36}O$, 280 g/mol) appeared as peak 29 with a RT of 87.40 min and an area of 1.06%.

Generally, GEO at 0 time exposure for UV-C had 8 major compounds which were : (+)-Sesamin [23.62) (lignin)]; 5-(1R,3aR,4 S,6aR)-4-(Benzo[d]$^{(1,3)}$ dioxol-5-yl) hexahydrofuro [3, 4-c] furan-1-yl) oxy) benzo [d]$^{(1,3)}$ dioxol; trans-13-Octadecenoic acid [(13.80) (Fatty acid)]; Trans 13-Octadecenoic acid [(7.72) (Fatty acid)]; 9-Octadecenoic acid ethyl ester [(7.14) (Fatty acid ester)] ; 9-Octadecenoic acid (Z)-, 2,3-dihydroxypropyl ester [(7.09) (Fatty acid ester)]; 9,12-Octadecadienoic acid (Z, Z)-, methyl ester [(4.95) (Fatty acid ester)]; n-Hexadecanoic acid [(4.30) (Fatty acid ester)]; 9,12-Octadecadienoic acid (Z, Z)-, 2-hydroxy-1-(hydroxymethyl) ethyl ester [(3.41) (Fatty acid ester)]. While, at 30 min exposure of UV-C had **9 major compounds** which

were: 9-Octadecadienoic acid, methyl ester [(14.26) (Fatty acid ester)]; Ethyl oleate [(13.17) (Fatty acid ester)]; 9,12-Octadecadienoic acid (Z, Z)-, methyl ester [(10.26) (Fatty acid ester)]; Ethyl (9Z,12Z)-9,12-octadecadienoate [(9.90) (Fatty acid ester)]; (+)-Sesamin [(9.75) (liginin)]; 9-Octadecenoic acid [(7.56) (Fatty acid)]; Oleic acid, 3-hydroxypropyl ester (5.75) (Fatty acid ester; Hexadecanoic acid, ethyl ester [(4.56) Fatty acid ester]; 5-(1R,3aR,4 S,6aR)-4-(Benzo[d]$^{(1,3)}$ dioxol-5-yl) hexahydrofuro [3, 4-c] furan-1-yl) oxy) benzo [d]$^{(1,3)}$ dioxol [(3.17) (Furan derivative)]. Lastly, GEO exposed for 60 min of UV-C had **7 major molecules** which were: Ethyl oleate [(13.62) (Fatty acid ester)]; 9-Octadecenoic acid [(13.52) (Fatty acid)]; 9-Octadecenoic acid, methyl ester [(10.91) (Fatty acid)], 9,12-Octadecadienoic acid (Z, Z)-, methyl ester [(8.68) (Fatty acid)]; (+)-Sesamin [(8.36) (lignin)]; 9-Octadecenoic acid (Z)-, 2,3-dihydroxypropyl ester [(4.81) (Fatty acid ester)]; 5-(1R,3aR,4 S,6aR)-4-(Benzo[d]$^{(1,3)}$ dioxol-5-yl) hexahydrofuro [3, 4-c] furan-1-yl) oxy) benzo [d]$^{(1,3)}$ dioxol [(3.25) (Furan derivative)]. Where these compounds were represented by their names, peak areas, and corresponding classes.

Lee et al.[34] reported that ginseng extract contained a limited number of components detectable by GC–MS analysis, with ginsenosides representing the compound of highest abundance. Xin-Hong et al.[39] highlighted that ginseng flowers possess significant therapeutic potential due to their rich content of bioactive compounds. The volatile organic compounds in ginseng flowers were analyzed by GC-MS, using four extraction methods, namely steam distillation, supercritical fluid extraction, headspace solid phase extraction, and static headspace sampling. There were 103 components annotated using the area normalization approach, highlighting the key differences between the four extraction methods. The main components, 1,6,10-dodecatriene, 7,11-dimethyl-3-methylene-, and (E)- were the only common components. The number of components identified by each method was 67, 20, 38, and 18 for steam distillation, supercritical fluid extraction, headspace solid-phase extraction, and static headspace sampling, respectively, corresponding to 89.67%, 61.84%, 82.6%, and 50.3% of the total volatile oil peak areas. Components present at proportions exceeding 1% numbered 11, 9, 8, and 8 for each method, respectively. Terpenoids were identified as the major volatile organic compounds in ginseng flowers, with steam distillation yielding the highest sesquiterpene content.

Ginseng contains a diverse array of bioactive compounds, with ginsenosides—triterpenoid saponin glycosides—being the most prominent. These compounds exhibit a broad spectrum of pharmacological effects, including antioxidant, antimicrobial, anticancer, and anti-inflammatory activities[40]. Beyond their therapeutic properties, ginseng extracts are widely used in cosmetic formulations, particularly in Korea and other regions, due to their potential to improve skin health[41]. In addition to ginsenosides, the volatile oil fraction of ginseng has been reported to possess cardioprotective effects and a variety of bioactivities, such as antibacterial, anti-aging, anti-platelet aggregation, and neuroprotective effects, largely mediated through anti-inflammatory and nutritional support mechanisms[42]. Moreover, recent studies indicate that ginseng may serve as a promising natural candidate for managing metabolic disorders, such as non-alcoholic fatty liver disease[43].

Conclusions and study limitations

The present study provides the comprehensive evidence that UV-C irradiation significantly enhances the bioactivity of ginseng oil extract (GOE). Comparative analyses revealed that UV-C–treated ginseng oil exhibited markedly improved antimicrobial and anti-biofilm activities against *B. subtilis*, *S. aureus*, *K. pneumoniae*, *S. typhi* and *C. albicans*. Moreover, the treated oil demonstrated superior inhibition of biofilm formation and disruption of established biofilms compared with the untreated counterpart. These effects were supported by GC–MS profiling, which indicated UV-C–induced modifications in the chemical composition, leading to the enrichment of bioactive constituents with known antibacterial and anti-inflammatory potential. Additionally, the UV-C–treated ginseng oil effectively stabilized red blood cell membranes in the anti-inflammatory assay, suggesting its potential as a natural anti-inflammatory agent. Although this study evaluated multiple biological activities of GOE under controlled in vitro conditions. However, several limitations should be considered. The antimicrobial effects were tested only against standard ATCC strains rather than clinical isolates, which may differ in resistance patterns. The study did not include cytotoxicity or biocompatibility assessments of GOE on mammalian cells, which are essential to confirm its safety for therapeutic use. Furthermore, the chemical changes induced by UV-C exposure were analyzed qualitatively but not quantitatively, limiting precise correlation between chemical composition and biological activity. In vivo studies and molecular investigations are still required to elucidate the exact mechanisms underlying GOE's enhanced antimicrobial and anti-inflammatory properties after UV-C treatment.

Data availability

The results from the present investigation are available from the corresponding author upon reasonable appeal.

Received: 31 May 2025; Accepted: 10 December 2025
Published online: 27 January 2026

References

1. Alsolami, A., Bazaid, A. S., Alshammari, M. A. & Abdelghany, T. M. Ecofriendly fabrication of natural Jojoba nanoemulsion and chitosan/jojoba nanoemulsion with antimicrobial, anti-biofilm, and anti-diabetic activities *in vitro*. *Biomass Convers. Bioref.* https://doi.org/10.1007/s13399-023-05162-0 (2023).
2. Almehayawi, M. S. et al. Evaluating the anti-yeast, anti-diabetic, wound-healing activities of *Moringa oleifera* extracted at different pressures via supercritical fluid extraction. *BioResources* **19**, 5961–5977. https://doi.org/10.15376/biores.19.3.5961-5977 (2024).
3. Alawlaqi, M. M., Al-Rajhi, A. M. H., Abdelghany, T. M., Ganash, M. & Moawad, H. Evaluation of biomedical applications for linseed extract: antimicrobial, antioxidant, anti-diabetic, and anti-inflammatory activities *in vitro*. *J. Funct. Biomater.* **14**, 300. https://doi.org/10.3390/jfb14060300 (2023).
4. Zanuso, B. O. et al. *Panax ginseng* and aging-related disorders: a systematic review. *Exp. Gerontol.* **161**, 111731 (2022).
5. Shim, H. et al. Dynamic evolution of *Panax* species. *Genes Genom.* **43**, 209–215 (2021).

6. Ogawa-Ochiai, K. & Kawasaki, K. *Panax ginseng* for frailty-related disorders: a review. *Front. Nutr.* **5**, 140 (2019).
7. Xu, J. et al. *Panax ginseng* genome examination for ginsenoside biosynthesis. *GigaScience* **6**, 1–15 (2017).
8. Shi, Z., Chen, H., Zhou, X., Yang, W. & Lin, Y. Pharmacological effects of natural medicine ginsenosides against alzheimer's disease. *Front. Pharmacol.* **13**, 952332 (2022).
9. Lan, T. et al. Ginsenoside Rb1 prevents homocysteine-induced endothelial dysfunction via PI3K/Akt activation and PKC Inhibition. *Biochem. Pharmacol.* **82**, 148–155 (2011).
10. Han, S. et al. AKT-targeted anti-inflammatory activity of *Panax ginseng* calyx ethanolic extract. *J. Ginseng Res.* **42**, 496–503 (2018).
11. Lee, D. Y. et al. Ginseng berry prevents alcohol-induced liver damage by improving the anti-inflammatory system in mice. *Int. J. Mol. Sci.* **20**, 3522 (2019).
12. Lee, J. I., Park, K. S. & Cho, I. H. *Panax ginseng*: a candidate herbal medicine for autoimmune disease. *J. Ginseng Res.* **43**, 342–348 (2019).
13. Yang, X., Xiong, X., Wang, H. & Wang, J. Protective effects of *Panax notoginseng* saponins on cardiovascular diseases: a comprehensive overview. *Evid.-Based Complement. Altern. Med.* 204840 (2014).
14. Zhao, Y. et al. Ginseng total saponin improves red blood cell oxidative stress injury by regulating tyrosine phosphorylation and Glycolysis. *Phytomedicine* **130**, 155785 (2024).
15. Bazaz, M. R., Rahman, Z., Qadir, I., Pasam, T. & Dandekar, M. P. Springer,. Importance of gut microbiome-based therapeutics in cancer treatment. In *Targeted Cancer Therapy in Biomedical Engineering* 831–885 (2023).
16. Duan, L., Dou, L. L., Guo, L., Li, P. & Liu, E. H. Comprehensive evaluation of deep eutectic solvents in extraction of bioactive natural products. *ACS Sustain. Chem. Eng.* **4**, 2405–2411 (2016).
17. Meresta, A. et al. Plant-derived pectin nanocoatings prevent inflammatory response of osteoblasts following *Porphyromonas gingivalis* infection. *Int. J. Nanomed.* **12**, 433 (2017).
18. Lee, M. H. et al. Quality and characteristics of ginseng seed oil treated using different extraction methods. *J. Ginseng Res.* **37**, 468–474 (2013).
19. Alsalamah, S. A. et al. Effect of UV-C radiation on chemical profile and pharmaceutical application in vitro of Aloe Vera oil. *AMB Express*. **15** (83). https://doi.org/10.1186/s13568-025-01884-8 (2025).
20. Magaldi, S. et al. Well diffusion for antifungal susceptibility testing. *Int. J. Infect. Dis.* **8**, 39–45 (2004).
21. Anna, M., Anna, G., Izabela, K. & Tomasz, B. Anti-*Helicobacter pylori* activity *in vitro* of chamomile, coneflower, peppermint, and thyme. *Curr. Issues Pharm. Med. Sci.* **28**, 30–32 (2015).
22. Chioma, A. A., Onyechi, O. & Lawrence, U. S. E. Membrane stabilization as a mechanism of anti-inflammatory activity of *Solanum aethiopicum*. *DARU J. Pharm. Sci.* **20**, 76 (2012).
23. Rossignol, G. et al. Involvement of phospholipase C in the hemolytic activity of *Pseudomonas fluorescens*. *BMC Microbiol.* **8**, 189 (2008).
24. Antunes, A. L. S. et al. Determination of biofilm antimicrobial susceptibility in Staphylococci. *APMIS* **118**, 873–877 (2010).
25. Niu, C. & Gilbert, E. S. Colorimetric method for identifying essential oil components affecting biofilm formation. *Appl. Environ. Microbiol.* **70**, 6951–6956 (2004).
26. Huwaimel, B. et al. Novel insights into phytochemical, biological, toxicological, and computational activities of *Satureja hortensis* L. *Food Chem. Toxicol.* **179**, 113969 (2023).
27. Mokhtar, F. Y., Nasr, A. E., Elaasser, M. M. & Elsaba, Y. M. Bioactive secondary metabolites from *Aspergillus fumigatus* ON428521 isolated from Wadi El Rayan, Egypt. *Egypt. J. Bot.* **63**, 233–250 (2023).
28. Khattab, O., El-Safey, A., Elaasser, M. & Bakry, W. GC–MS separation of bioactive fraction from *Aspergillus flavus* isolated from El-Qussair marine environments. *Egypt. J. Bot.* **62**, 747–762 (2022).
29. Wang, L. et al. Antimicrobial activities of Asian ginseng, American ginseng, and Notoginseng. *Phytother Res.* **34**, 1–11 (2019).
30. Soyuçok, A., Kılıç, B., Kılıç, G. B. & Yalçın, H. *In vitro* antimicrobial activity of ginseng extract against foodborne pathogens. *Meat Sci.* **216**, 109559 (2024).
31. Soyoung, N., Jin-Hee, K. & Young, K. R. Se-Wook, O. Enhancing antimicrobial activity of ginseng against *Bacillus cereus* and *Staphylococcus aureus* by heat treatment. *Food Sci. Biotechnol.* **27**, 203–210 (2018).
32. Manzanelli, F. A. et al. Enhancing the functional properties of tea tree oil: *in vitro* antimicrobial activity and microencapsulation strategy. *Pharmaceutics* **15**, 2489. https://doi.org/10.3390/pharmaceutics15102489 (2023).
33. Campana, R. et al. Comparative analysis of the antimicrobial activity of essential oils and their microemulsions against foodborne pathogens. *Antibiotics* **11**, 447 (2022).
34. Lee, C., Lee, S., Jang, Y. P. & Park, J. Anti-inflammatory activity of vacuum distillate from *Panax ginseng* root on LPS-induced RAW264.7 cells. *J. Microbiol. Biotechnol.* **34**, 262–269 (2024).
35. Angeloni, S. et al. Anti-inflammatory and antioxidant activities of ginsenosides and ginseng root extract to counteract obesity. *Eur. Food Res. Technol.* **250**, 119–133 (2023).
36. Enad, H. H. & Nahidh, M. Salivary cortisol as a stress biomarker and total viable count of oral microbiota among COVID-19 patients. *J. Baghdad Coll. Dent.* **33**, 6–10 (2021).
37. Kadhum, W. N. & Al-Ogaidi, I. A. Z. Evaluation of chitosan–alginate nanoparticle as a stable antibacterial formula in biological fluids. *Iraqi J. Sci.* **63**, 2398–2418 (2022).
38. Ermolenko, E., Koroleva, I., Suvorov, A. Microbial Therapy with Indigenous Bacteria: From Idea toClinical Evidence. In: Boyko, N., Golubnitschaja, O. (eds) Microbiome in 3P Medicine Strategies. *Advances in Predictive, Preventiveand Personalised Medicine*, **16**. Springer, Cham. https://doi.org/10.1007/978-3-031-19564-8_9 (2023).
39. Xin-Hong, S. et al. Comparative analysis of volatile components of *Panax ginseng* flower by four extraction methods. *Chin. J. Anal. Chem.* **52**, 100366 (2024).
40. Mehta, D. S., Rathore, P. & Rai, G. Ginseng: Pharmacological action and phytochemistry prospective. In Ginseng in Medicine (Working Title) (IntechOpen, London, https://doi.org/10.5772/intechopen.99646 (2021).
41. Kim, J. H. et al. Ginseng and ginseng byproducts for skincare and skin health. *J. Ginseng Res.* **48**, 525–534. https://doi.org/10.1016/j.jgr.2024.09.006 (2024).
42. Xu, Y. et al. Phytochemistry, Pharmacological effects and mechanism of action of volatile oil from *Panax ginseng*: a review. *Front. Pharmacol.* **15**, 1436624. https://doi.org/10.3389/fphar.2024.1436624 (2024).
43. Hao, L. et al. Therapeutic potential of ginseng and its bioactive components in nonalcoholic fatty liver disease. *Drug Des. Devel Ther.* **19**, 83–96. https://doi.org/10.2147/DDDT.S500719 (2025).

Acknowledgements

Princess Nourah bint Abdulrahman University Researchers Supporting Project number (PNURSP2026R217), Princess Nourah bint Abdulrahman University, Riyadh, Saudi Arabia.

Author contributions

Methodology and Conceptualization, A.M.H.A. and A.M.A.; Formal analysis and Writing—review and editing, N.M.A, S.A.A., R.Y., A. A. A., and M. H.; All authors have read and agreed to the published version of the manuscript.

Funding
This research was funded by Princess Nourah bint Abdulrahman University Researchers Supporting Project number (PNURSP2026R217), Princess Nourah bint Abdulrahman University, Riyadh, Saudi Arabia.

Declarations

Competing interests
The authors declare no competing interests.

Guidelines
All methods were carried out in accordance with relevant guidelines and regulations All experimental protocols were approved at No: HAP-01-R-059 by viaInstitutional Review Board (IRB), Graduate Studies and Scientific Research Vice- Rectorate, Princess Nourah bint Abdulrahman University, Riyadh, KSA.

Additional information
Correspondence and requests for materials should be addressed to S.A.A.

Reprints and permissions information is available at www.nature.com/reprints.

Publisher's note Springer Nature remains neutral with regard to jurisdictional claims in published maps and institutional affiliations.